

Photonic penguins at two loops and m_t -dependence of $BR[B \rightarrow X_s l^+ l^-]$

Christoph Bobeth¹, Mikołaj Misiak^{2,3,4} and Jörg Urban^{1,2}

¹*Institut für Theoretische Physik, Technische Universität Dresden,
Mommsenstr. 13, D-01062 Dresden, Germany*

²*Physik Department, Technische Universität München,
D-85748 Garching, Germany*

³*Institute of Theoretical Physics, Warsaw University,
Hoża 69, PL-00-681 Warsaw, Poland*

⁴*Theory Division, CERN, CH-1211 Geneva 23, Switzerland*

Abstract

We calculate two-loop matching conditions for all the operators that are relevant to $B \rightarrow X_s l^+ l^-$ decay in the Standard Model. In effect, we are able to remove the $\pm 16\%$ uncertainty in the decay spectrum, which was mainly due to the renormalization-scale dependence of the top-quark mass. We find 1.46×10^{-6} for the branching ratio integrated in the domain $m_{l^+ l^-}^2/m_b^2 \in [0.05, 0.25]$, for $l = e$ or μ . There remains around 13% perturbative uncertainty in this quantity, while the non-perturbative effects are expected to be smaller.

1 Introduction

The forthcoming measurement of the inclusive decay mode $B \rightarrow X_s l^+ l^-$ is expected to provide an important test of possible new physics effects at the electroweak scale. However, the existing theoretical predictions for the branching ratio in the Standard Model (SM) still suffer from many uncertainties, some of which are larger than the expected experimental errors.

The most important theoretical uncertainties are due to intermediate $c\bar{c}$ states. Because of the non-perturbative nature of these states, the differential decay spectrum can be only roughly estimated when the invariant mass of the lepton pair $m_{l^+l^-}^2$ is not significantly below $m_{J/\psi}$. It remains questionable whether integrating the decay rate over this domain can reduce the theoretical uncertainty below $\pm 20\%$ [1].

On the contrary, for low $\hat{s} = m_{l^+l^-}^2/m_{b,pole}^2$ (accessible to $l = e$ or μ), a relatively precise determination of the decay spectrum is possible using perturbative methods only, up to calculable HQET corrections. The dominant HQET corrections were evaluated in refs. [2]–[6] and found to be small (smaller than 6% for $0.05 < \hat{s} < 0.25$). Effects of similar size are found in this region when purely perturbative expressions for $c\bar{c}$ contributions are compared with the ones obtained via dispersion relations in the factorization approximation (see fig. 1 in section 4). Thus, the $B \rightarrow X_s l^+ l^-$ decay rate integrated over this region of \hat{s} should be perturbatively predictable as precisely as the $B \rightarrow X_s \gamma$ decay rate, i.e. up to about 10% uncertainty.

Unfortunately, the presently available perturbative calculations [7, 8] have not yet reached this precision, even though they are performed at the next-to-leading (NLO) order in QCD. The formally leading-order term is (quite accidentally) suppressed, which makes it as small as some of the NLO contributions. Consequently, some of the formally next-to-next-to-leading (NNLO) terms can have an effect larger than 10% on the differential decay rate. It can be easily verified by varying the renormalization scale at which the top quark mass is renormalized in the formulae of refs. [7, 8].

The formalism of effective theories, which is conventionally used in the analyses of weak B decays, allows the identification of three types of NNLO contributions to $B \rightarrow X_s l^+ l^-$. The first type originates from two-loop matching between the Standard Model and the effective

theory amplitudes, i.e. to two-loop contributions to the Wilson coefficients in the effective theory at the scale $\mu_0 \sim M_W$. The second type is due to the three-loop renormalization group evolution of the Wilson coefficients down to the scale $\mu_b \sim m_b$. The third type originates from two-loop matrix elements of the effective theory operators between the physical states of interest. One should include one-loop Bremsstrahlung corrections as well. Performing a complete NNLO calculation is thus a very involved task.

In the present paper, we shall calculate only the first type of corrections, i.e. those originating from the two-loop matching conditions. Our results will allow us to remove the significant uncertainty of the former NLO prediction stemming from the dependence on the scale μ_0 . The remaining uncalculated NNLO effects will be estimated in section 4.

Our paper is organized as follows. In section 2, we introduce the effective theory and present a complete set of the matching conditions up to two loops. The resulting formulae for the so-called effective coefficients are given in section 3. Section 4 is devoted to discussing phenomenological implications of our results for $B \rightarrow X_s l^+ l^-$. Technical details of the matching computation are relegated to section 5. There, one can find an extensive description of the two-loop matching procedure for the photonic penguin diagrams, which has been the most involved original part of our calculation. Section 5 can serve as a practical guide for performing any two-loop matching computation, not necessarily in the domain of flavour physics.

2 Summary of the two-loop matching conditions

The effective theory lagrangian relevant to $B \rightarrow X_s l^+ l^-$ decay has the following form

$$\begin{aligned}
\mathcal{L}_{eff} &= \mathcal{L}_{QCD \times QED}(u, d, s, c, b, e, \mu, \tau) \\
&+ \frac{4G_F}{\sqrt{2}} [V_{us}^* V_{ub} (C_1^c P_1^u + C_2^c P_2^u) + V_{cs}^* V_{cb} (C_1^c P_1^c + C_2^c P_2^c)] \\
&+ \frac{4G_F}{\sqrt{2}} \sum_{i=3}^{10} [(V_{us}^* V_{ub} + V_{cs}^* V_{cb}) C_i^c + V_{ts}^* V_{tb} C_i^t] P_i.
\end{aligned} \tag{1}$$

For further convenience, we refrain from using unitarity of the CKM matrix \hat{V} in all the analytical formulae here. The first term in eq. (1) consists of kinetic terms of the light SM particles as well as their QCD and QED interactions. The remaining two terms consist of

$\Delta B = -\Delta S = 1$ local operators of dimension ≤ 6 , built out of those light fields:¹

$$\begin{aligned}
P_1^u &= (\bar{s}_L \gamma_\mu T^a u_L)(\bar{u}_L \gamma^\mu T^a b_L), \\
P_2^u &= (\bar{s}_L \gamma_\mu u_L)(\bar{u}_L \gamma^\mu b_L), \\
P_1^c &= (\bar{s}_L \gamma_\mu T^a c_L)(\bar{c}_L \gamma^\mu T^a b_L), \\
P_2^c &= (\bar{s}_L \gamma_\mu c_L)(\bar{c}_L \gamma^\mu b_L), \\
P_3 &= (\bar{s}_L \gamma_\mu b_L) \sum_q (\bar{q} \gamma^\mu q), \\
P_4 &= (\bar{s}_L \gamma_\mu T^a b_L) \sum_q (\bar{q} \gamma^\mu T^a q), \\
P_5 &= (\bar{s}_L \gamma_{\mu_1} \gamma_{\mu_2} \gamma_{\mu_3} b_L) \sum_q (\bar{q} \gamma^{\mu_1} \gamma^{\mu_2} \gamma^{\mu_3} q), \\
P_6 &= (\bar{s}_L \gamma_{\mu_1} \gamma_{\mu_2} \gamma_{\mu_3} T^a b_L) \sum_q (\bar{q} \gamma^{\mu_1} \gamma^{\mu_2} \gamma^{\mu_3} T^a q), \\
P_7 &= \frac{e}{g^2} m_b (\bar{s}_L \sigma^{\mu\nu} b_R) F_{\mu\nu}, \\
P_8 &= \frac{1}{g} m_b (\bar{s}_L \sigma^{\mu\nu} T^a b_R) G_{\mu\nu}^a, \\
P_9 &= \frac{e^2}{g^2} (\bar{s}_L \gamma_\mu b_L) \sum_l (\bar{l} \gamma^\mu l), \\
P_{10} &= \frac{e^2}{g^2} (\bar{s}_L \gamma_\mu b_L) \sum_l (\bar{l} \gamma^\mu \gamma_5 l),
\end{aligned} \tag{2}$$

where sums over q and l denote sums over all the light quarks and all the leptons, respectively.

The Wilson coefficients can be perturbatively expanded as follows

$$C_i^Q = C_i^{Q(0)} + \frac{g^2}{(4\pi)^2} C_i^{Q(1)} + \frac{g^4}{(4\pi)^4} C_i^{Q(2)} + \mathcal{O}(g^6), \quad Q = c \text{ or } t. \tag{3}$$

Their values are found in the matching procedure, which amounts to requiring equality of $b \rightarrow s+(\text{light particles})$ Green functions calculated in the effective theory and in the full Standard Model, up to $\mathcal{O}[(\text{external momenta and light masses})^2/M_W^2]$. Contributions of order g^{2n} to each Wilson coefficient originate from n -loop SM diagrams, which follows from the particular convention for powers of gauge couplings in the normalization of our operators.

Dimensional regularization with fully anticommuting γ_5 has been used in our matching computation. Using this simple scheme could not cause any difficulties, because the choice of the four-quark operator basis in eq. (2) allowed us to avoid the appearance of Dirac traces containing γ_5 in the effective theory diagrams [9]. No such traces were present in the SM diagrams, either.

The \overline{MS} scheme with scale $\mu_0 \sim M_W$ was used for all the QCD counterterms, both in

¹ The s -quark mass is neglected here, i.e. it is assumed to be negligibly small when compared to m_b . Of course, no such assumption is made concerning m_c or m_τ .

the SM and in the effective theory.² In addition, several non-physical operators had to be included on the effective theory side, because the calculation was performed off-shell (see section 5 and the appendix for details).

The 't Hooft–Feynman version of the background field gauge was used for all the gauge bosons. It allowed us to perform the matching without making use of the CKM-matrix unitarity.

The only relevant off-shell electroweak counterterm (on the SM side) proportional to $\bar{s}\not{D}b$ was taken in the MOM scheme, at $q^2 = 0$ for the $\bar{s}\not{D}b$ term, and at vanishing external momenta for the terms containing gauge bosons.

The obtained matching conditions are the following. At the tree level, all the $C_i^{Q(0)}$ vanish, except for

$$C_2^{c(0)} = -1. \quad (4)$$

The one- and two-loop matching conditions are summarized below:

$$\begin{aligned}
C_1^{c(1)} &= -15 - 6L, \\
C_2^{c(1)} &= 0, \\
C_3^{c(1)} &= 0, & C_3^{t(1)} &= 0, \\
C_4^{c(1)} &= \frac{7}{9} - \frac{2}{3}L, & C_4^{t(1)} &= E_0^t(x), \\
C_5^{c(1)} &= 0, & C_5^{t(1)} &= 0, \\
C_6^{c(1)} &= 0, & C_6^{t(1)} &= 0, \\
C_7^{c(1)} &= \frac{23}{36}, & C_7^{t(1)} &= -\frac{1}{2}A_0^t(x), \\
C_8^{c(1)} &= \frac{1}{3}, & C_8^{t(1)} &= -\frac{1}{2}F_0^t(x), \\
C_9^{c(1)} &= -\frac{1}{4s_w^2} - \frac{38}{27} + \frac{4}{9}L, & C_9^{t(1)} &= \frac{1-4s_w^2}{s_w^2}C_0^t(x) - \frac{1}{s_w^2}B_0^t(x) - D_0^t(x), \\
C_{10}^{c(1)} &= \frac{1}{4s_w^2}, & C_{10}^{t(1)} &= \frac{1}{s_w^2}[B_0^t(x) - C_0^t(x)], \\
\\
C_1^{c(2)} &= T(x) - \frac{7987}{72} - \frac{17}{3}\pi^2 - \frac{475}{6}L - 17L^2, \\
C_2^{c(2)} &= -\frac{127}{18} - \frac{4}{3}\pi^2 - \frac{46}{3}L - 4L^2, \\
C_3^{c(2)} &= \frac{680}{243} + \frac{20}{81}\pi^2 + \frac{68}{81}L + \frac{20}{27}L^2, & C_3^{t(2)} &= G_1^t(x), \\
C_4^{c(2)} &= -\frac{950}{243} - \frac{10}{81}\pi^2 - \frac{124}{27}L - \frac{10}{27}L^2, & C_4^{t(2)} &= E_1^t(x),
\end{aligned}$$

² The only exceptions were the top-quark-loop contributions to the renormalization of the light-quark and gluon wave functions on the SM side. The corresponding terms in the propagators were subtracted in the MOM scheme at $q^2 = 0$. In consequence, no top-quark loop contribution remained in the (W-boson)–(light quark) effective vertex after renormalization.

$$\begin{aligned}
C_5^{c(2)} &= -\frac{68}{243} - \frac{2}{81}\pi^2 - \frac{14}{81}L - \frac{2}{27}L^2, & C_5^{t(2)} &= -\frac{1}{10}G_1^t(x) + \frac{2}{15}E_0^t(x), \\
C_6^{c(2)} &= -\frac{85}{162} - \frac{5}{108}\pi^2 - \frac{35}{108}L - \frac{5}{36}L^2, & C_6^{t(2)} &= -\frac{3}{16}G_1^t(x) + \frac{1}{4}E_0^t(x), \\
C_7^{c(2)} &= -\frac{713}{243} - \frac{4}{81}L, & C_7^{t(2)} &= -\frac{1}{2}A_1^t(x), \\
C_8^{c(2)} &= -\frac{91}{324} + \frac{4}{27}L, & C_8^{t(2)} &= -\frac{1}{2}F_1^t(x), \\
C_9^{c(2)} &= -\frac{1}{s_w^2} - \frac{524}{729} + \frac{128}{243}\pi^2 + \frac{16}{3}L + \frac{128}{81}L^2, & C_9^{t(2)} &= \frac{1-4s_w^2}{s_w^2}C_1^t(x) - \frac{1}{s_w^2}B_1^t(x, -\frac{1}{2}) - D_1^t(x), \\
C_{10}^{c(2)} &= \frac{1}{s_w^2}, & C_{10}^{t(2)} &= \frac{1}{s_w^2} \left[B_1^t(x, -\frac{1}{2}) - C_1^t(x) \right],
\end{aligned}$$

where

$$x = \left(\frac{m_t \overline{MS}(\mu_0)}{M_W} \right)^2, \quad L = \ln \frac{\mu_0^2}{M_W^2}, \quad s_w = \sin \theta_w \quad (5)$$

and

$$A_0^t(x) = \frac{-3x^3+2x^2}{2(1-x)^4} \ln x + \frac{22x^3-153x^2+159x-46}{36(1-x)^3}, \quad (6)$$

$$B_0^t(x) = \frac{x}{4(1-x)^2} \ln x + \frac{1}{4(1-x)}, \quad (7)$$

$$C_0^t(x) = \frac{3x^2+2x}{8(1-x)^2} \ln x + \frac{-x^2+6x}{8(1-x)}, \quad (8)$$

$$D_0^t(x) = \frac{-3x^4+30x^3-54x^2+32x-8}{18(1-x)^4} \ln x + \frac{-47x^3+237x^2-312x+104}{108(1-x)^3}, \quad (9)$$

$$E_0^t(x) = \frac{-9x^2+16x-4}{6(1-x)^4} \ln x + \frac{-7x^3-21x^2+42x+4}{36(1-x)^3}, \quad (10)$$

$$F_0^t(x) = \frac{3x^2}{2(1-x)^4} \ln x + \frac{5x^3-9x^2+30x-8}{12(1-x)^3}, \quad (11)$$

$$\begin{aligned}
A_1^t(x) &= \frac{32x^4+244x^3-160x^2+16x}{9(1-x)^4} Li_2 \left(1 - \frac{1}{x} \right) + \frac{-774x^4-2826x^3+1994x^2-130x+8}{81(1-x)^5} \ln x \\
&+ \frac{-94x^4-18665x^3+20682x^2-9113x+2006}{243(1-x)^4} \\
&+ \left[\frac{-12x^4-92x^3+56x^2}{3(1-x)^5} \ln x + \frac{-68x^4-202x^3-804x^2+794x-152}{27(1-x)^4} \right] \ln \frac{\mu_0^2}{m_t^2}, \quad (12)
\end{aligned}$$

$$B_1^t(x, -\frac{1}{2}) = \frac{-2x}{(1-x)^2} Li_2 \left(1 - \frac{1}{x} \right) + \frac{-x^2+17x}{3(1-x)^3} \ln x + \frac{13x+3}{3(1-x)^2} + \left[\frac{2x^2+2x}{(1-x)^3} \ln x + \frac{4x}{(1-x)^2} \right] \ln \frac{\mu_0^2}{m_t^2}, \quad (13)$$

$$\begin{aligned}
C_1^t(x) &= \frac{-x^3-4x}{(1-x)^2} Li_2 \left(1 - \frac{1}{x} \right) + \frac{3x^3+14x^2+23x}{3(1-x)^3} \ln x + \frac{4x^3+7x^2+29x}{3(1-x)^2} \\
&+ \left[\frac{8x^2+2x}{(1-x)^3} \ln x + \frac{x^3+x^2+8x}{(1-x)^2} \right] \ln \frac{\mu_0^2}{m_t^2}, \quad (14)
\end{aligned}$$

$$\begin{aligned}
D_1^t(x) &= \frac{380x^4-1352x^3+1656x^2-784x+256}{81(1-x)^4} Li_2 \left(1 - \frac{1}{x} \right) + \frac{304x^4+1716x^3-4644x^2+2768x-720}{81(1-x)^5} \ln x \\
&+ \frac{-6175x^4+41608x^3-66723x^2+33106x-7000}{729(1-x)^4} \\
&+ \left[\frac{648x^4-720x^3-232x^2-160x+32}{81(1-x)^5} \ln x + \frac{-352x^4+4912x^3-8280x^2+3304x-880}{243(1-x)^4} \right] \ln \frac{\mu_0^2}{m_t^2}, \quad (15)
\end{aligned}$$

$$\begin{aligned}
E_1^t(x) &= \frac{515x^4-614x^3-81x^2-190x+40}{54(1-x)^4} Li_2 \left(1 - \frac{1}{x} \right) + \frac{-1030x^4+435x^3+1373x^2+1950x-424}{108(1-x)^5} \ln x \\
&+ \frac{-29467x^4+45604x^3-30237x^2+66532x-10960}{1944(1-x)^4}
\end{aligned}$$

$$+ \left[\frac{-1125x^3+1685x^2+380x-76}{54(1-x)^5} \ln x + \frac{133x^4-2758x^3-2061x^2+11522x-1652}{324(1-x)^4} \right] \ln \frac{\mu_0^2}{m_t^2}, \quad (16)$$

$$\begin{aligned} F_1^t(x) &= \frac{4x^4-40x^3-41x^2-x}{3(1-x)^4} Li_2\left(1-\frac{1}{x}\right) + \frac{-144x^4+3177x^3+3661x^2+250x-32}{108(1-x)^5} \ln x \\ &+ \frac{-247x^4+11890x^3+31779x^2-2966x+1016}{648(1-x)^4} \\ &+ \left[\frac{17x^3+31x^2}{(1-x)^5} \ln x + \frac{-35x^4+170x^3+447x^2+338x-56}{18(1-x)^4} \right] \ln \frac{\mu_0^2}{m_t^2}, \end{aligned} \quad (17)$$

$$\begin{aligned} G_1^t(x) &= \frac{10x^4-100x^3+30x^2+160x-40}{27(1-x)^4} Li_2\left(1-\frac{1}{x}\right) + \frac{30x^3-42x^2-332x+68}{81(1-x)^4} \ln x \\ &+ \frac{-6x^3-293x^2+161x+42}{81(1-x)^3} + \left[\frac{90x^2-160x+40}{27(1-x)^4} \ln x + \frac{35x^3+105x^2-210x-20}{81(1-x)^3} \right] \ln \frac{\mu_0^2}{m_t^2}, \end{aligned} \quad (18)$$

$$T(x) = -(16x+8)\sqrt{4x-1} Cl_2\left(2 \arcsin \frac{1}{2\sqrt{x}}\right) + \left(16x + \frac{20}{3}\right) \ln x + 32x + \frac{112}{9}. \quad (19)$$

The integral representations for the functions Li_2 and Cl_2 are as follows:

$$Li_2(z) = - \int_0^z dt \frac{\ln(1-t)}{t}, \quad (20)$$

$$Cl_2(x) = \text{Im} [Li_2(e^{ix})] = - \int_0^x d\theta \ln |2 \sin(\theta/2)|. \quad (21)$$

Our matching results for all the $C_k^{Q(2)}$ are new, except for $k = 7, 8$ and 10 . In the cases $k = 7$ and $k = 8$, we agree with the previously published results [10]. The $k = 10$ case has already been discussed by us in ref. [11], and the original calculation [12] has been corrected in ref. [13].

3 The effective coefficients

Once the matching conditions are found, the Wilson coefficients should be evolved from $\mu_0 \sim M_W$ to $\mu_b \sim m_b$, according to the Renormalization Group Equation (RGE)

$$\mu \frac{d}{d\mu} \vec{C}^Q = (\hat{\gamma}^Q)^T \vec{C}^Q, \quad (22)$$

which has the following general solution

$$\vec{C}^Q(\mu_b) = \hat{U}^Q(\mu_b, \mu_0) \vec{C}^Q(\mu_0), \quad (23)$$

where

$$\begin{aligned} \hat{U}^Q(\mu_b, \mu_0) &= T_g \exp \int_{g(\mu_0)}^{g(\mu_b)} dg' \frac{(\hat{\gamma}^Q(g'))^T}{\beta(g')} \\ &= \hat{U}^{Q(0)}(\mu_b, \mu_0) + \frac{\alpha_s(\mu_0)}{4\pi} \hat{U}^{Q(1)}(\mu_b, \mu_0) + \frac{\alpha_s(\mu_0)^2}{(4\pi)^2} \hat{U}^{Q(2)}(\mu_b, \mu_0) + \dots \end{aligned} \quad (24)$$

In the intermediate step of the above equation, T_g denotes ordering of the coupling constants such that they increase from right to left.

The anomalous dimension matrices $\hat{\gamma}^Q$ have the following perturbative expansion

$$\hat{\gamma}^Q = \frac{\alpha_s}{4\pi} \hat{\gamma}^{Q(0)} + \frac{\alpha_s^2}{(4\pi)^2} \hat{\gamma}^{Q(1)} + \frac{\alpha_s^3}{(4\pi)^3} \hat{\gamma}^{Q(2)} + \dots \quad (25)$$

The one- and two-loop anomalous dimension matrices have already been evaluated in refs. [7, 8]. However, transforming them to the “new” operator basis (2) is quite non-trivial (see ref. [9] for the 6×6 submatrix). In the “new” basis (and in the \overline{MS} scheme with the evanescent operators specified in the appendix), the matrices $\hat{\gamma}^{c(0)}$ and $\hat{\gamma}^{c(1)}$ read³

$$\hat{\gamma}^{c(0)} = \begin{pmatrix} -4 & \frac{8}{3} & 0 & -\frac{2}{9} & 0 & 0 & 0 & 0 & -\frac{32}{27} & 0 \\ 12 & 0 & 0 & \frac{4}{3} & 0 & 0 & 0 & 0 & -\frac{8}{9} & 0 \\ 0 & 0 & 0 & -\frac{52}{3} & 0 & 2 & 0 & 0 & -\frac{16}{9} & 0 \\ 0 & 0 & -\frac{40}{9} & -\frac{100}{9} & \frac{4}{9} & \frac{5}{6} & 0 & 0 & \frac{32}{27} & 0 \\ 0 & 0 & 0 & -\frac{256}{3} & 0 & 20 & 0 & 0 & -\frac{112}{9} & 0 \\ 0 & 0 & -\frac{256}{9} & \frac{56}{9} & \frac{40}{9} & -\frac{2}{3} & 0 & 0 & \frac{512}{27} & 0 \\ 0 & 0 & 0 & 0 & 0 & 0 & \frac{32}{3} - 2\beta_0 & 0 & 0 & 0 \\ 0 & 0 & 0 & 0 & 0 & 0 & -\frac{32}{9} & \frac{28}{3} - 2\beta_0 & 0 & 0 \\ 0 & 0 & 0 & 0 & 0 & 0 & 0 & 0 & -2\beta_0 & 0 \\ 0 & 0 & 0 & 0 & 0 & 0 & 0 & 0 & 0 & -2\beta_0 \end{pmatrix}, \quad (26)$$

$$\hat{\gamma}^{c(1)} = \begin{pmatrix} -\frac{355}{9} & -\frac{502}{27} & -\frac{1412}{243} & -\frac{1369}{243} & \frac{134}{243} & -\frac{35}{162} & -\frac{232}{243} & \frac{167}{162} & -\frac{2272}{729} & 0 \\ -\frac{35}{3} & -\frac{28}{3} & -\frac{416}{81} & \frac{1280}{81} & \frac{56}{81} & \frac{35}{27} & \frac{464}{81} & \frac{76}{27} & \frac{1952}{243} & 0 \\ 0 & 0 & -\frac{4468}{81} & -\frac{31469}{81} & \frac{400}{81} & \frac{3373}{108} & \frac{64}{81} & \frac{368}{27} & -\frac{6752}{243} & 0 \\ 0 & 0 & -\frac{8158}{243} & -\frac{59399}{243} & \frac{269}{486} & \frac{12899}{648} & -\frac{200}{243} & -\frac{1409}{162} & -\frac{2192}{729} & 0 \\ 0 & 0 & -\frac{251680}{81} & -\frac{128648}{81} & \frac{23836}{81} & \frac{6106}{27} & -\frac{6464}{81} & \frac{13052}{27} & -\frac{84032}{243} & 0 \\ 0 & 0 & \frac{58640}{243} & -\frac{26348}{243} & -\frac{14324}{243} & -\frac{2551}{162} & -\frac{11408}{243} & -\frac{2740}{81} & -\frac{37856}{729} & 0 \\ 0 & 0 & 0 & 0 & 0 & 0 & \frac{4688}{27} - 2\beta_1 & 0 & 0 & 0 \\ 0 & 0 & 0 & 0 & 0 & 0 & -\frac{2192}{81} & \frac{4063}{27} - 2\beta_1 & 0 & 0 \\ 0 & 0 & 0 & 0 & 0 & 0 & 0 & 0 & -2\beta_1 & 0 \\ 0 & 0 & 0 & 0 & 0 & 0 & 0 & 0 & 0 & -2\beta_1 \end{pmatrix}, \quad (27)$$

³ Note that the matrices given here correspond to the normalization of operators P_7, \dots, P_{10} as in eq. (2) and to their ordinary Wilson coefficients, not to the so-called “effective” ones that will be introduced below.

where $\beta_0 = \frac{23}{3}$ and $\beta_1 = \frac{116}{3}$. The analogous matrices $\hat{\gamma}^{t(0)}$ and $\hat{\gamma}^{t(1)}$ can be obtained from the ones above by removing the first two rows and the first two columns.

The complete NNLO prediction for $BR[B \rightarrow X_s l^+ l^-]$ depends on two entries of $\hat{U}^{c(2)}(\mu_b, \mu_0)$, i.e. on $U_{72}^{c(2)}(\mu_b, \mu_0)$ and $U_{92}^{c(2)}(\mu_b, \mu_0)$ that are generated by the three-loop matrix $\hat{\gamma}^{c(2)}$. Unfortunately, the only entries of $\hat{\gamma}^{c(2)}$ that have been calculated so far are the ones corresponding to the mixing $\{P_1, \dots, P_6\} \rightarrow \{P_7, P_8\}$ [14]. Therefore, $U_{72}^{c(2)}(\mu_b, \mu_0)$ is known but $U_{92}^{c(2)}(\mu_b, \mu_0)$ is not. Below, we shall include the unknown $U_{92}^{c(2)}(\mu_b, \mu_0)$ in our analytical formulae. Its potential numerical relevance will be tested in the next section.

After performing the RGE evolution, one evaluates the perturbative expression for $d\Gamma[b \rightarrow X_s l^+ l^-]/d\hat{s}$. It amounts to calculating perturbative matrix elements of the operators P_i among the external partonic on-shell states, multiplying them by the appropriate Wilson coefficients and performing the phase-space integrals. At NLO, one obtains [7, 8]:

$$\begin{aligned} \frac{d\Gamma(b \rightarrow X_s l^+ l^-)}{d\hat{s}} &= \frac{G_F^2 m_{b,pole}^5 |V_{ts}^* V_{tb}|^2}{48\pi^3} \left(\frac{\alpha_{em}}{4\pi}\right)^2 (1 - \hat{s})^2 \times \\ &\times \left\{ (1 + 2\hat{s}) \left(|\tilde{C}_9^{eff}(\hat{s})|^2 + |\tilde{C}_{10}^{eff}(\hat{s})|^2 \right) + 4 \left(1 + \frac{2}{\hat{s}} \right) (\tilde{C}_7^{eff})^2 + 12\tilde{C}_7^{eff} \text{Re}(\tilde{C}_9^{eff}(\hat{s})) \right\}. \end{aligned} \quad (28)$$

The quantities \tilde{C}_k^{eff} can be split into top- and light-quark contributions:

$$\tilde{C}_k^{eff} = \tilde{C}_k^{teff} + \frac{V_{cs}^* V_{cb}}{V_{ts}^* V_{tb}} \tilde{C}_k^{ceff} + \frac{V_{us}^* V_{ub}}{V_{ts}^* V_{tb}} \left(\tilde{C}_k^{ceff} + \delta_{k9} \Delta \tilde{C}_9^{eff} \right) \quad (29)$$

that are related to the evolved coefficients $C_k^Q(\mu_b)$ as follows:

$$\tilde{C}_7^{Qeff} = \frac{4\pi}{\alpha_s(\mu_b)} C_7^Q(\mu_b) - \frac{1}{3} C_3^Q(\mu_b) - \frac{4}{9} C_4^Q(\mu_b) - \frac{20}{3} C_5^Q(\mu_b) - \frac{80}{9} C_6^Q(\mu_b), \quad (30)$$

$$\begin{aligned} \tilde{C}_9^{Qeff}(\hat{s}) &= 4C_9^Q(\mu_b) \left(\frac{\pi}{\alpha_s(\mu_b)} + \omega(\hat{s}) \right) + \sum_{i=1}^6 C_i^Q(\mu_b) \gamma_{i9}^{Q(0)} \ln \frac{m_b}{\mu_b} \\ &+ h \left(\frac{m_c^2}{m_b^2}, \hat{s} \right) \left[\left(\frac{4}{3} C_1^c(\mu_b) + C_2^c(\mu_b) \right) \delta_{Qc} + 6C_3^Q(\mu_b) + 60C_5^Q(\mu_b) \right] \\ &+ h(1, \hat{s}) \left(-\frac{7}{2} C_3^Q(\mu_b) - \frac{2}{3} C_4^Q(\mu_b) - 38C_5^Q(\mu_b) - \frac{32}{3} C_6^Q(\mu_b) \right) \\ &+ h(0, \hat{s}) \left(-\frac{1}{2} C_3^Q(\mu_b) - \frac{2}{3} C_4^Q(\mu_b) - 8C_5^Q(\mu_b) - \frac{32}{3} C_6^Q(\mu_b) \right) \\ &+ \frac{4}{3} C_3^Q(\mu_b) + \frac{64}{9} C_5^Q(\mu_b) + \frac{64}{27} C_6^Q(\mu_b), \end{aligned} \quad (31)$$

$$\tilde{C}_{10}^{Qeff}(\hat{s}) = 4C_{10}^Q(\mu_b) \left(\frac{\pi}{\alpha_s(\mu_b)} + \omega(\hat{s}) \right), \quad (32)$$

$$\Delta \tilde{C}_9^{eff} = \left[h(0, \hat{s}) - h \left(\frac{m_c^2}{m_b^2}, \hat{s} \right) \right] \left(\frac{4}{3} C_1^c(\mu_b) + C_2^c(\mu_b) \right), \quad (33)$$

where

$$\begin{aligned}
h(z, \hat{s}) &= -\frac{4}{9} \ln z + \frac{8}{27} + \frac{4}{9}x - \frac{2}{9}(2+x)\sqrt{|1-x|} \begin{cases} \ln \left| \frac{\sqrt{1-x+1}}{\sqrt{1-x-1}} \right| - i\pi, & \text{for } x \equiv 4z/\hat{s} < 1, \\ 2 \arctan(1/\sqrt{x-1}), & \text{for } x \equiv 4z/\hat{s} > 1, \end{cases} \\
\omega(\hat{s}) &= -\frac{4}{3} Li_2(\hat{s}) - \frac{2}{3} \ln(1-\hat{s}) \ln \hat{s} - \frac{2}{9} \pi^2 - \frac{5+4\hat{s}}{3(1+2\hat{s})} \ln(1-\hat{s}) \\
&\quad - \frac{2\hat{s}(1+\hat{s})(1-2\hat{s})}{3(1-\hat{s})^2(1+2\hat{s})} \ln \hat{s} + \frac{5+9\hat{s}-6\hat{s}^2}{6(1-\hat{s})(1+2\hat{s})}. \tag{34}
\end{aligned}$$

Calculating the differential decay rate with the help of eq. (28), one *must* retain only terms linear in $\omega(\hat{s})$ and also set $\omega(\hat{s})$ to zero in the interference term proportional to $\text{Re}(C_9^{eff}(\hat{s}))$.

The coefficients multiplying C_1^Q, \dots, C_6^Q in eqs. (30) and (31) are different from the corresponding ones in refs. [7, 8], because we use a different operator basis here.

Substituting the evolved Wilson coefficients to eqs. (30)–(33), we obtain the following expressions for the “effective coefficients”:

$$\tilde{C}_7^{c\,eff} = -\sum_{i=1}^8 \eta^{a_i} \left[h_i^c + \frac{\alpha_s(\mu_0)}{4\pi} \left(\frac{h_i^{c(-)}}{\eta} + h_i^{c'} + h_i^{cL} L \right) \right], \tag{35}$$

$$\begin{aligned}
\tilde{C}_7^{t\,eff} &= -\frac{1}{2} \eta^{\frac{16}{23}} A_0^t(x) + \frac{4}{3} (\eta^{\frac{16}{23}} - \eta^{\frac{14}{23}}) F_0^t(x) + \frac{\alpha_s(\mu_0)}{4\pi} \left[E_0^t(x) \sum_{i=1}^8 e_i^t \eta^{a_i} \right. \\
&\quad - \frac{1}{2} \eta^{\frac{16}{23}} A_1^t(x) + \frac{4}{3} (\eta^{\frac{16}{23}} - \eta^{\frac{14}{23}}) F_1^t(x) + \frac{18604}{4761} (\eta^{-\frac{7}{23}} - \eta^{\frac{16}{23}}) A_0^t(x) \\
&\quad \left. + \left(\frac{3582208}{357075} \eta^{-\frac{9}{23}} - \frac{148832}{14283} \eta^{-\frac{7}{23}} - \frac{128434}{14283} \eta^{\frac{14}{23}} + \frac{3349442}{357075} \eta^{\frac{16}{23}} \right) F_0^t(x) \right], \tag{36}
\end{aligned}$$

$$\begin{aligned}
\tilde{C}_9^{c\,eff}(\hat{s}) &= -\left(\frac{\pi}{\alpha_s(\mu_0)} + \frac{\omega(\hat{s})}{\eta} \right) \sum_{i=3}^9 p_i^{c(+)} \eta^{a_i+1} - \frac{1}{4s_w^2} \\
&\quad - \sum_{i=3}^9 \eta^{a_i} \left[r_i^c + r_i^{c(+)} \eta + r_i^{cL(+)} \eta L + s_i^c \ln \frac{m_b}{\mu_b} + t_i^c h \left(\frac{m_c^2}{m_b^2}, \hat{s} \right) + u_i^c h(1, \hat{s}) + w_i^c h(0, \hat{s}) \right] \\
&\quad - \frac{\alpha_s(\mu_0)}{4\pi} \left\{ U_{92}^{c(2)}(\mu_b, \mu_0) + \frac{\eta + \omega(\hat{s})}{\eta s_w^2} + \sum_{i=3}^9 \eta^{a_i} \left[r_i^{cT(+)} \eta T(x) + \frac{r_i^{c(-)}}{\eta} + r_i^{c'} + r_i^{c(+)} \eta \right. \right. \\
&\quad \left. \left. + (r_i^{cL} + r_i^{cL(+)} \eta) L + r_i^{cL^2(+)} \eta L^2 + r_i^{c\pi^2(+)} \eta \pi^2 + \left(\frac{r_i^{c\omega(-)}}{\eta} + r_i^{c(+)} + r_i^{cL(+)} L \right) 4\omega(\hat{s}) \right. \right. \\
&\quad \left. \left. + \left(\frac{s_i^{c(-)}}{\eta} + s_i^{c'} + s_i^{cL} L \right) \ln \frac{m_b}{\mu_b} + \left(\frac{t_i^{c(-)}}{\eta} + t_i^{c'} + t_i^{cL} L \right) h \left(\frac{m_c^2}{m_b^2}, \hat{s} \right) \right. \right. \\
&\quad \left. \left. + \left(\frac{u_i^{c(-)}}{\eta} + u_i^{c'} + u_i^{cL} L \right) h(1, \hat{s}) + \left(\frac{w_i^{c(-)}}{\eta} + w_i^{c'} + w_i^{cL} L \right) h(0, \hat{s}) \right] \right\}, \tag{37}
\end{aligned}$$

$$\begin{aligned}
\tilde{C}_9^{t\,eff}(\hat{s}) &= \left[\frac{1 - 4s_w^2}{s_w^2} C_0^t(x) - \frac{1}{s_w^2} B_0^t(x) - D_0^t(x) \right] \left(1 + \frac{\alpha_s(\mu_0)}{\pi} \frac{\omega(\hat{s})}{\eta} \right) \\
&+ \left[E_0^t(x) + \frac{\alpha_s(\mu_0)}{4\pi} \left(E_1^t(x) + \frac{4\omega(\hat{s})}{\eta} E_0^t(x) \right) \right] \sum_{i=5}^9 q_i^{t(+)} \eta^{a_i+1} \\
&+ \frac{\alpha_s(\mu_0)}{4\pi} \left\{ \frac{1 - 4s_w^2}{s_w^2} C_1^t(x) - \frac{1}{s_w^2} B_1^t(x, -\frac{1}{2}) - D_1^t(x) + G_1^t(x) \sum_{i=5}^9 y_i^{t(+)} \eta^{a_i+1} \right. \\
&\left. + E_0^t(x) \sum_{i=5}^9 \eta^{a_i} \left[r_i^{t'} + r_i^{t(+)} \eta + s_i^{t'} \ln \frac{m_b}{\mu_b} + t_i^{t'} h \left(\frac{m_c^2}{m_b^2}, \hat{s} \right) + u_i^{t'} h(1, \hat{s}) + w_i^{t'} h(0, \hat{s}) \right] \right\}, \quad (38)
\end{aligned}$$

$$\tilde{C}_{10}^{c\,eff}(\hat{s}) = \frac{1}{4s_w^2} \left[1 + \frac{\alpha_s(\mu_0)}{\pi} \left(1 + \frac{\omega(\hat{s})}{\eta} \right) \right], \quad (39)$$

$$\tilde{C}_{10}^{t\,eff}(\hat{s}) = \frac{1}{s_w^2} \left\{ B_0^t(x) - C_0^t(x) + \frac{\alpha_s(\mu_0)}{4\pi} \left[B_1^t(x) - C_1^t(x) + \frac{4\omega(\hat{s})}{\eta} (B_0^t(x) - C_0^t(x)) \right] \right\}, \quad (40)$$

$$\begin{aligned}
\Delta \tilde{C}_9^{eff} &= \left[h(0, \hat{s}) - h \left(\frac{m_c^2}{m_b^2}, \hat{s} \right) \right] \left\{ -2\eta^{\frac{6}{23}} + \eta^{-\frac{12}{23}} + \frac{\alpha_s(\mu_0)}{4\pi} \left[-\frac{15745}{1587} \eta^{-\frac{17}{23}} \right. \right. \\
&\left. \left. - \frac{151}{1587} \eta^{-\frac{35}{23}} - \frac{6473}{1587} \eta^{\frac{6}{23}} - \frac{9371}{1587} \eta^{-\frac{12}{23}} - 4L \left(\eta^{\frac{6}{23}} + \eta^{-\frac{12}{23}} \right) \right] \right\}, \quad (41)
\end{aligned}$$

where $\eta = \alpha_s(\mu_0)/\alpha_s(\mu_b)$ and $a_i = (\frac{14}{23}, \frac{16}{23}, \frac{6}{23}, -\frac{12}{23}, 0.4086, -0.4230, -0.8994, 0.1456, -1)_i$.

The ‘‘magic numbers’’ entering the above expressions are collected in tables 1, 2 and 3.

It is straightforward to verify that our results for the $\mathcal{O}(1/\alpha_s)$ and $\mathcal{O}(1)$ parts of \tilde{C}_9^{eff} and \tilde{C}_{10}^{eff} are identical to the ones found in refs. [7, 8]. Only the $\mathcal{O}(\alpha_s)$ parts are new here. As far as \tilde{C}_7^{eff} is concerned, we just reproduce the result of ref. [14], where the $\mathcal{O}(\alpha_s)$ part was already present.

In order to obtain the complete NLO prediction for the $B \rightarrow X_s l^+ l^-$ decay rate, one should

i	1	2	3	4	5	6	7	8
h_i^c	$\frac{42678}{30253}$	$-\frac{86697}{103460}$	$-\frac{3}{7}$	$-\frac{1}{14}$	-0.6494	-0.0380	-0.0186	-0.0057
$h_i^{c(-)}$	$-\frac{4246707584}{400095925}$	$\frac{89606166}{13682585}$	$\frac{45043984}{9898119}$	$\frac{34505657}{45891279}$	2.0040	0.7476	-0.5385	0.0914
$h_i^{t'c}$	$\frac{3344583818789933}{360615755431797}$	$-\frac{90790555261878016}{13088650734603675}$	$-\frac{6473}{7406}$	$\frac{9371}{22218}$	-2.7231	0.4083	0.1465	0.0205
$h_i^{t'cL}$	$\frac{199164}{30253}$	$-\frac{115596}{25865}$	$-\frac{6}{7}$	$\frac{2}{7}$	-2.0343	0.1232	0.1279	-0.0064
$e_i^{t'}$	$\frac{4298158}{816831}$	$-\frac{8516}{2217}$	0	0	-1.9043	-0.1008	0.1216	0.0183

Table 1. ‘‘Magic numbers’’ entering the expressions for $\tilde{C}_7^{c\,eff}$ and $\tilde{C}_7^{t\,eff}$. Three-loop anomalous dimensions from ref. [14] have been used in their evaluation.

i	3	4	5	6	7	8	9
$p_i^{c(+)}$	$-\frac{80}{203}$	$\frac{8}{33}$	0.0433	0.1384	0.1648	-0.0073	$-\frac{4704688}{25088393}$
r_i^c	$\frac{3085}{3703}$	$-\frac{129}{1058}$	-0.1642	0.0793	-0.0451	-0.1638	0
$r_i^{c(+)}$	$-\frac{64730}{322161}$	$-\frac{18742}{52371}$	0.0454	-0.3719	-0.3254	0.0066	$\frac{1775737}{809303}$
$r_i^{cL(+)}$	$-\frac{40}{203}$	$-\frac{8}{33}$	0.0339	-0.1122	-0.2841	-0.0020	$\frac{27051956}{75265179}$
$r_i^{cT(+)}$	$\frac{20}{609}$	$\frac{4}{99}$	-0.0021	0.0289	0.0174	0.0010	$-\frac{8908520}{75265179}$
$r_i^{c(-)}$	$-\frac{316900}{299943}$	$\frac{51388}{128547}$	1.9957	-0.8153	0.1488	-0.2353	0
$r_i^{c'}$	$\frac{183859}{42849}$	$\frac{130739}{128547}$	-0.0939	-0.9763	0.0393	-2.2799	0
$r_i^{c(+)}$	$-\frac{8129495}{5798898}$	$-\frac{4447705}{942678}$	0.6261	-3.6869	0.2246	0.0121	$\frac{4896690443}{677386611}$
r_i^{cL}	$\frac{6170}{3703}$	$\frac{258}{529}$	-0.5145	-0.2571	0.3111	-0.1829	0
$r_i^{cL(+)}$	$-\frac{97850}{33327}$	$-\frac{398258}{157113}$	0.6618	-2.2108	-1.6839	0.0472	$\frac{4704688}{2595351}$
$r_i^{cL^2(+)}$	$-\frac{20}{21}$	$-\frac{4}{9}$	0.1833	-0.2481	-0.1096	-0.0090	0
$r_i^{c\pi^2(+)}$	$-\frac{20}{63}$	$-\frac{4}{27}$	0.0611	-0.0827	-0.0365	-0.0030	0
$r_i^{c\omega(-)}$	$\frac{87527}{99981}$	$-\frac{6217}{85698}$	-0.1685	0.0323	-0.0475	-0.2018	0
s_i^c	$-\frac{40}{21}$	$\frac{4}{9}$	0.2340	0.3061	0.0636	-0.0322	0
$s_i^{c(-)}$	$-\frac{1373012}{128547}$	$-\frac{735748}{385641}$	2.1605	0.3356	0.8434	-0.2456	0
$s_i^{c'}$	$-\frac{129460}{33327}$	$-\frac{37484}{14283}$	0.9813	-3.2900	-0.5020	0.1151	0
s_i^{cL}	$-\frac{80}{21}$	$-\frac{16}{9}$	0.7330	-0.9925	-0.4383	-0.0359	0
t_i^c	$\frac{12}{7}$	$-\frac{2}{3}$	0.1658	-0.2407	-0.0717	0.0990	0
$t_i^{c(-)}$	$\frac{33606}{3703}$	$-\frac{6046}{4761}$	-0.1681	1.2986	-0.3397	0.4766	0
$t_i^{c'}$	$\frac{12946}{3703}$	$\frac{18742}{4761}$	0.6951	2.5871	0.5664	-0.3540	0
t_i^{cL}	$\frac{24}{7}$	$\frac{8}{3}$	0.5193	0.7805	0.4945	0.1106	0
u_i^c	$\frac{2}{7}$	0	-0.2559	0.0083	0.0180	-0.0562	0
$u_i^{c(-)}$	$\frac{168155}{99981}$	$\frac{166}{81}$	-1.0892	-1.1627	-0.2197	-0.2193	0
$u_i^{c'}$	$\frac{6473}{11109}$	0	-1.0733	-0.0897	-0.1424	0.2008	0
u_i^{cL}	$\frac{4}{7}$	0	-0.8018	-0.0271	-0.1243	-0.0627	0
w_i^c	$\frac{1}{7}$	$\frac{1}{6}$	-0.1731	-0.1120	-0.0178	-0.0067	0
$w_i^{c(-)}$	$\frac{251737}{199962}$	$\frac{117137}{85698}$	-1.1732	-0.5134	-0.3895	0.0190	0
$w_i^{c'}$	$\frac{6473}{22218}$	$-\frac{9371}{9522}$	-0.7257	1.2038	0.1408	0.0238	0
w_i^{cL}	$\frac{2}{7}$	$-\frac{2}{3}$	-0.5421	0.3632	0.1229	-0.0074	0

Table 2. “Magic numbers” entering the expression for $\tilde{C}_9^{c\,eff}$.

i	5	6	7	8	9
$q_i^{t(+)}$	0.0318	0.0918	-0.2700	0.0059	$\frac{33160}{235941}$
$r_i^{t'}$	-0.4817	0.2104	0.2956	0.5246	0
$r_i^{t(+)}$	0.2164	-0.4330	-0.9126	0.0660	$\frac{6672596}{12976755}$
$s_i^{t'}$	0.6862	0.8125	-0.4165	0.1031	0
$t_i^{t'}$	0.4861	-0.6389	0.4699	-0.3171	0
$u_i^{t'}$	-0.7505	0.0221	-0.1182	0.1799	0
$w_i^{t'}$	-0.5075	-0.2973	0.1168	0.0213	0
$y_i^{t(+)}$	-0.1242	-0.0956	-0.1628	-0.0176	$\frac{157366}{393235}$

Table 3. “Magic numbers” entering the expression for $\tilde{C}_9^{t\,eff}$.

use eqs. (28)–(33) and neglect the $\mathcal{O}(\alpha_s)$ contributions to the effective coefficients $\tilde{C}_k^{Q\,eff}(\hat{s})$ (i.e. include only the $\mathcal{O}(1/\alpha_s)$ and $\mathcal{O}(1)$ parts of them). On the other hand, in the complete NNLO calculation, it is *not* sufficient to take into account the $\mathcal{O}(\alpha_s)$ parts of the effective coefficients. One should also modify eq. (28) by including effects originating e.g. from two-loop matrix elements of the four-quark operators and the corresponding Bremsstrahlung corrections.

In the present paper, we are able to include the NNLO effects only partly. We shall simply use eq. (28), but at the same time we will include the $\mathcal{O}(\alpha_s)$ contributions to the effective coefficients. In this way, we will include all the m_t -dependent NNLO contributions to the branching ratio,⁴ as well as the terms enhanced by $1/s_w^2 \sim 4.3$. It is important to calculate the m_t -dependent terms at the NNLO level, because both $C_9^t(\mu_0)$ and $C_{10}^t(\mu_0)$ grow with m_t in the formal limit $m_t \rightarrow \infty$. Therefore, $m_t^2/M_W^2 \sim 4.8$ plays the role of an enhancement factor, too.

Above, we have presented explicitly all the $\mathcal{O}(\alpha_s)$ parts of the effective coefficients. However, the unknown quantity $U_{92}^{c(2)}(\mu_b, \mu_0)$ occurred in $\tilde{C}_9^{c\,eff}(\hat{s})$. In our numerical calculations described in the next section, it will be assumed that $U_{92}^{c(2)}(\mu_b, \mu_0)$ vanishes. We shall relax this assumption below eq. (49), and check that the expected numerical effect of $U_{92}^{c(2)}(\mu_b, \mu_0)$ on the decay rate is very small.

⁴ The only exceptions are the m_t -dependent contributions from the one-loop matrix elements of P_7 and P_8 . However, they are proportional to the relatively small Wilson coefficients $C_7(\mu_b)$ and $C_8(\mu_b)$ that do not grow with m_t in the formal limit $m_t \rightarrow \infty$.

4 Phenomenological implications

In the present section, we shall study the numerical importance of the calculated NNLO effects as well as the uncertainties due to the yet unknown contributions.

As a first step, let us calculate the effective coefficients for several different values of μ_0 and μ_b . We will vary μ_b by a factor of 2 around $m_b \sim 5$ GeV, i.e. we will take $\mu_b = 2.5, 5$ and 10 GeV. In the expressions for $\tilde{C}_k^{c\,eff}$ and $\Delta\tilde{C}_9^{eff}$, we will vary μ_0 by a factor of 2 around $M_W \sim 80$ GeV, i.e. we will take $\mu_0 = 40, 80$ and 160 GeV. In the expressions for $\tilde{C}_k^{t\,eff}$, we will vary μ_0 by a factor of 2 around $\sqrt{M_W m_t} \sim 120$ GeV, i.e. we will take $\mu_0 = 60, 120$ and 240 GeV.

The remaining input parameters will be equal to [15]

$$\alpha_s(M_Z) = 0.119, \quad m_t^{pole} = 173.8 \text{ GeV}, \quad M_W = 80.41 \text{ GeV}, \quad s_w^2 = 0.23124.$$

Since we shall keep \hat{s} arbitrary, our expressions for $\tilde{C}_9^{Q\,eff}$, $\tilde{C}_{10}^{Q\,eff}$ and $\Delta\tilde{C}_9^{eff}$ will read

$$\tilde{C}_9^{Q\,eff} = A_9^Q + R_9^Q \omega(\hat{s}) + T_9^Q h\left(\frac{m_c^2}{m_b^2}, \hat{s}\right) + U_9^Q h(1, \hat{s}) + W_9^Q h(0, \hat{s}), \quad (42)$$

$$\tilde{C}_{10}^{Q\,eff} = A_{10}^Q + R_{10}^Q \omega(\hat{s}), \quad (43)$$

$$\Delta\tilde{C}_9^{eff} = Z_9 \left[h(0, \hat{s}) - h\left(\frac{m_c^2}{m_b^2}, \hat{s}\right) \right]. \quad (44)$$

The coefficients A_k^Q, \dots, W_k^Q are independent of m_c , and they only weakly depend on m_b via the logarithm $\ln(m_b/\mu_b)$. In this logarithm, we shall use $m_b = 4.8$ GeV.

In tables 4 and 5, our results for $\tilde{C}_7^{Q\,eff}$, A_k^Q, \dots, W_k^Q and Z_9 are given, both with and without the $\mathcal{O}(\alpha_s)$ contributions. They allow the following observations:

- The dominant contributions to the “effective coefficients” and to the decay rate originate from A_9^c and A_{10}^t . However, the coefficients $\tilde{C}_7^{Q\,eff}$ are not much less important, because of the factor “12” in the last term of eq. (28).
- The inclusion of the $\mathcal{O}(\alpha_s)$ contributions significantly reduces the μ_0 -dependence. It is especially important in the case of A_{10}^t , which had varied by more than $\pm 10\%$ before including the $\mathcal{O}(\alpha_s)$ correction. The dependence on μ_0 remains significant only in the relatively small quantities such as R_{10}^t . (R_{10}^t is multiplied by $\omega(\hat{s}) \in [-1.32, -1.24]$ for $\hat{s} \in [0.05, 0.25]$).

μ_0 [GeV]	40	80	160	80	80
μ_b [GeV]	5	5	5	2.5	10
$\alpha_s(\mu_0)$	0.136	0.121	0.110	0.121	0.121
$\alpha_s(\mu_b)$	0.215	0.215	0.215	0.267	0.180
η	0.633	0.565	0.510	0.454	0.674
$\tilde{C}_7^{c\,eff}$ with $\mathcal{O}(\alpha_s)$	0.567	0.567	0.566	0.554	0.579
$\tilde{C}_7^{c\,eff}$ without $\mathcal{O}(\alpha_s)$	0.631	0.631	0.632	0.634	0.631
A_9^c with $\mathcal{O}(\alpha_s)$	-4.685	-4.683	-4.689	-4.612	-4.828
A_9^c without $\mathcal{O}(\alpha_s)$	-4.620	-4.635	-4.681	-4.750	-4.635
A_9^c only $\mathcal{O}(1/\alpha_s)$	-1.569	-1.964	-2.315	-2.181	-1.612
R_9^c with $\mathcal{O}(\alpha_s)$	-0.315	-0.316	-0.320	-0.415	-0.242
R_9^c without $\mathcal{O}(\alpha_s)$	-0.107	-0.134	-0.158	-0.186	-0.092
T_9^c with $\mathcal{O}(\alpha_s)$	-0.641	-0.625	-0.603	-0.393	-0.807
T_9^c without $\mathcal{O}(\alpha_s)$	-0.505	-0.374	-0.255	-0.115	-0.576
U_9^c with $\mathcal{O}(\alpha_s)$	-0.048	-0.050	-0.052	-0.070	-0.035
U_9^c without $\mathcal{O}(\alpha_s)$	-0.026	-0.032	-0.038	-0.045	-0.022
W_9^c with $\mathcal{O}(\alpha_s)$	-0.045	-0.046	-0.047	-0.062	-0.033
W_9^c without $\mathcal{O}(\alpha_s)$	-0.026	-0.032	-0.038	-0.044	-0.022
A_{10}^c with $\mathcal{O}(\alpha_s)$	1.128	1.123	1.119	1.123	1.123
A_{10}^c without $\mathcal{O}(\alpha_s)$	1.081	1.081	1.081	1.081	1.081
R_{10}^c with $\mathcal{O}(\alpha_s)$	0.074	0.074	0.074	0.092	0.062
R_{10}^c without $\mathcal{O}(\alpha_s)$	0	0	0	0	0
Z_9 with $\mathcal{O}(\alpha_s)$	-0.648	-0.634	-0.613	-0.410	-0.811
Z_9 without $\mathcal{O}(\alpha_s)$	-0.506	-0.376	-0.257	-0.118	-0.577

Table 4. $\tilde{C}_7^{c\,eff}$, A_k^c , ..., W_k^c and Z_9 for various values of μ_0 and μ_b .

- The dependence on μ_b remains rather strong in most of the listed quantities. It follows mainly from the fact that two-loop matrix elements of the four-quark operators have not been included. It is relevant especially to the cases of $C_7^{t\,eff}$, T_9^c and R_9^c , which will cause considerable μ_b -dependence of the final prediction for the decay rate.
- The coefficients W_9^c turn out to be very small, while $\Delta\tilde{C}_9^{c\,eff}$ in eq. (29) is multiplied by $|(V_{us}^*V_{ub})/(V_{ts}^*V_{tb})| \simeq 0.08$. In consequence, the terms containing $h(0, \hat{s})$ contribute by less than 3% to the differential decay rate for $\hat{s} > 0.05$, because $|h(0, \hat{s})| = |\frac{8}{27} - \frac{4}{9}(\ln \hat{s} - i\pi)|$ is smaller than 2.2 in this region. This is fortunate, because $h(0, \hat{s})$ is expected to receive huge non-perturbative contributions from intermediate light hadron states.⁵ The smallness of W_9^c and V_{ub} allows us to use only the perturbative expression for $h(0, \hat{s})$ below. We could equivalently just neglect it.

⁵ These contributions are expected to be of the same size as $h(0, \hat{s})$ itself, after taking an average over a sufficiently wide region of \hat{s} .

μ_0 [GeV]	60	120	240	120	120
μ_b [GeV]	5	5	5	2.5	10
$m_t^{MS}(\mu_0)$ [GeV]	180	170	162	170	170
$\alpha_s(\mu_0)$	0.127	0.114	0.104	0.114	0.114
$\alpha_s(\mu_b)$	0.215	0.215	0.215	0.267	0.180
η	0.591	0.531	0.483	0.427	0.635
$\tilde{C}_7^{t\,eff}$ with $\mathcal{O}(\alpha_s)$	0.261	0.265	0.266	0.225	0.300
$\tilde{C}_7^{t\,eff}$ without $\mathcal{O}(\alpha_s)$	0.325	0.310	0.297	0.274	0.344
A_9^t with $\mathcal{O}(\alpha_s)$	-0.547	-0.541	-0.544	-0.541	-0.542
A_9^t without $\mathcal{O}(\alpha_s)$	-0.425	-0.506	-0.579	-0.509	-0.504
R_9^t with $\mathcal{O}(\alpha_s)$	-0.029	-0.035	-0.040	-0.043	-0.029
R_9^t without $\mathcal{O}(\alpha_s)$	0	0	0	0	0
T_9^t with $\mathcal{O}(\alpha_s)$	0.0002	0.0003	0.0004	0.0005	0.0001
T_9^t without $\mathcal{O}(\alpha_s)$	0	0	0	0	0
U_9^t with $\mathcal{O}(\alpha_s)$	-0.002	-0.002	-0.002	-0.002	-0.002
U_9^t without $\mathcal{O}(\alpha_s)$	0	0	0	0	0
W_9^t with $\mathcal{O}(\alpha_s)$	-0.002	-0.002	-0.002	-0.002	-0.002
W_9^t without $\mathcal{O}(\alpha_s)$	0	0	0	0	0
A_{10}^t with $\mathcal{O}(\alpha_s)$	-3.051	-3.115	-3.107	-3.115	-3.115
A_{10}^t without $\mathcal{O}(\alpha_s)$	-3.688	-3.292	-2.964	-3.292	-3.292
R_{10}^t with $\mathcal{O}(\alpha_s)$	-0.252	-0.225	-0.203	-0.280	-0.189
R_{10}^t without $\mathcal{O}(\alpha_s)$	0	0	0	0	0

Table 5. $\tilde{C}_7^{t\,eff}$ and A_k^t, \dots, W_k^t for various values of μ_0 and μ_b .

Huge non-perturbative contributions occur in $h(m_c^2/m_b^2, \hat{s})$ as well, for $\hat{s} > (2m_c/m_b)^2$. It is illustrated in fig. 1. Dashed lines show the real and imaginary parts of $h(z, \hat{s})$ from eq. (34), with $z = (1.4/4.8)^2$ and with $h(z, 0)$ subtracted. Solid lines present non-perturbative estimates of the same quantities obtained using the formulae and parameters from ref. [16] where the factorization approximation and dispersion relations were used.⁶

While the solid lines in fig. 1 should not be regarded as the true non-perturbative results (because of the factorization approximation), they give us qualitative information on the size of expected non-perturbative effects. In particular, we can observe that replacing the solid lines by the dashed ones in the region $\hat{s} \in [0.05, 0.25]$ should have quite a small effect on the predicted differential decay rate, owing to the relatively small size of T_9^Q in tables 4 and 5. Actually, the μ_b -dependence of T_9^c is numerically more important. Our aim below will be predicting the decay rate integrated over \hat{s} from 0.05 to 0.25. We shall use the purely perturbative expression for $h(z, \hat{s})$, keeping in mind that the μ_b -dependence of our prediction

⁶ However $4m_D^2$ is replaced by $4m_\pi^2$ in eq. (3.4) of ref. [16]. We thank F. Krüger for confirming that this was a misprint.

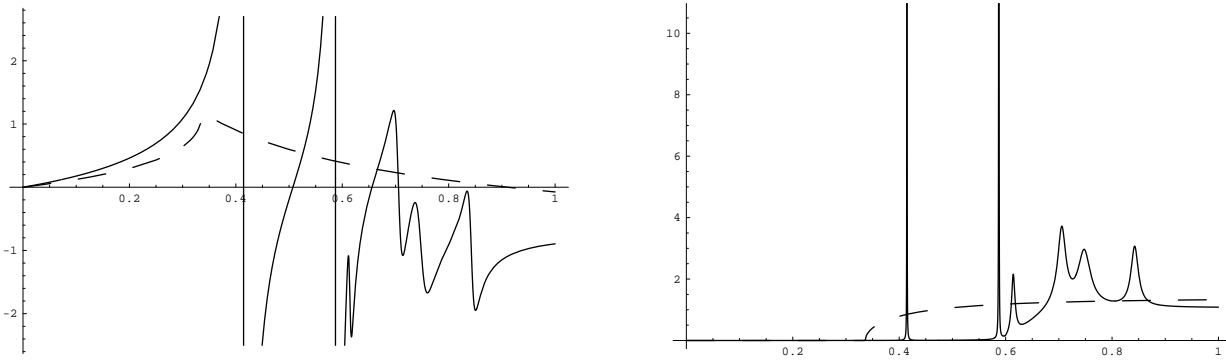


Figure 1: Perturbative and non-perturbative versions of $\text{Re}[h(m_c^2/m_b^2, \hat{s}) - h(m_c^2/m_b^2, 0)]$ and $\text{Im}[h(m_c^2/m_b^2, \hat{s}) - h(m_c^2/m_b^2, 0)]$ as functions of \hat{s} (see the text).

is expected to be larger than the uncertainty stemming from neglected non-perturbative effects.⁷

As far as $h(1, \hat{s})$ is concerned, the argument for using the purely perturbative expression can be the same as for $h(0, \hat{s})$ (small coefficients) or the same as for $h(m_c^2/m_b^2, \hat{s})$ (convergence of the perturbative and non-perturbative results for small \hat{s}).

The decay rate given in eq. (28) suffers from large uncertainties due to $m_{b,pole}^5$ and the CKM angles. One can get rid of them by normalizing to the semileptonic decay rate of the b -quark

$$\Gamma[b \rightarrow X_c e \bar{\nu}_e] = \frac{G_F^2 m_{b,pole}^5 |V_{cb}|^2 g \left(\frac{m_{c,pole}^2}{m_{b,pole}^2} \right) \kappa \left(\frac{m_c^2}{m_b^2} \right)}{192\pi^3}, \quad (45)$$

where

$$g(z) = 1 - 8z + 8z^3 - z^4 - 12z^2 \ln z \quad (46)$$

is the phase-space factor, and

$$\kappa(z) = 1 - \frac{2\alpha_s(m_b) h(z)}{3\pi g(z)} \quad (47)$$

is a sizeable next-to-leading order QCD correction to the semileptonic decay [17]. The function $h(z)$ has been given analytically in ref. [18]:

$$h(z) = -(1-z^2) \left(\frac{25}{4} - \frac{239}{3}z + \frac{25}{4}z^2 \right) + z \ln z \left(20 + 90z - \frac{4}{3}z^2 + \frac{17}{3}z^3 \right) + z^2 \ln^2 z (36 + z^2) \\ + (1-z^2) \left(\frac{17}{3} - \frac{64}{3}z + \frac{17}{3}z^2 \right) \ln(1-z) - 4(1+30z^2+z^4) \ln z \ln(1-z)$$

⁷ The non-perturbative effects estimated in fig. 1 are not included in the HQET correction we shall take into account later.

$$-(1 + 16z^2 + z^4)[6\text{Li}_2(z) - \pi^2] - 32z^{3/2}(1+z) \left[\pi^2 - 4\text{Li}_2(\sqrt{z}) + 4\text{Li}_2(-\sqrt{z}) - 2 \ln z \ln \left(\frac{1 - \sqrt{z}}{1 + \sqrt{z}} \right) \right].$$

Thus, the final perturbative quantity we consider is the ratio

$$R_{quark}^{l^+l^-}(\hat{s}) = \frac{1}{\Gamma[b \rightarrow X_c e \bar{\nu}_e]} \frac{d}{d\hat{s}} \Gamma(b \rightarrow X_s l^+ l^-). \quad (48)$$

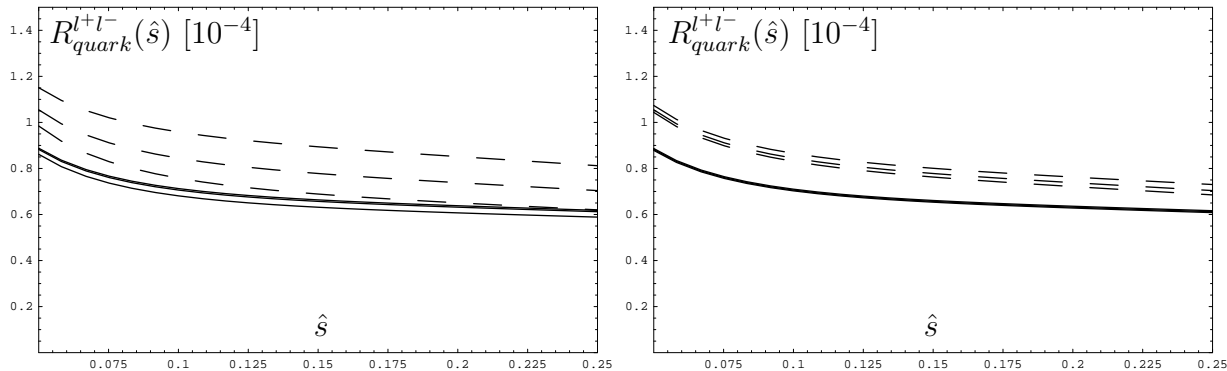


Figure 2: Reduction of μ_0 -dependence of $R_{quark}^{l^+l^-}(\hat{s})$.

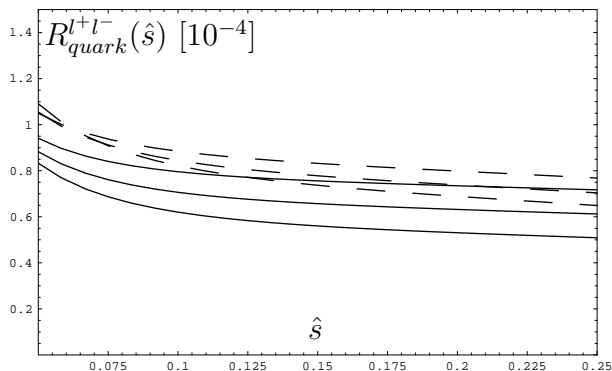


Figure 3: Remaining μ_b -dependence of $R_{quark}^{l^+l^-}(\hat{s})$.

Our results for $R_{quark}^{l^+l^-}(\hat{s})$ in the domain $\hat{s} \in [0.05, 0.25]$ are presented in figs. 2 and 3. In their evaluation, we have used $\alpha_{em} = \alpha_{em}(m_b \sqrt{0.15}) = \frac{1}{133}$ and $|V_{ts}^* V_{tb} / V_{cb}| = 0.976$. The quantity $\Delta \tilde{C}_9^{eff}$ that is multiplied by V_{ub} has been neglected. The dashed lines represent the pure NLO results, i.e. the ones with neglected $\mathcal{O}(\alpha_s)$ parts of the effective coefficients. The solid lines are obtained after including the $\mathcal{O}(\alpha_s)$ terms. Some of them overlap, and look like thick lines.

In both plots of fig. 2, $\mu_b = 5$ GeV, and three different values of μ_0 are chosen. The left plot corresponds to varying μ_0 by a factor of 2 around $\sqrt{M_W m_t}$ in $\tilde{C}_k^{t\,eff}$ (as in the first three columns of table 5) and keeping it fixed to M_W in $\tilde{C}_k^{c\,eff}$. The right plot corresponds

to varying μ_0 by a factor of 2 around M_W in $\tilde{C}_k^{c\,eff}$ (as in the first three columns of table 4) and keeping it fixed to $\sqrt{M_W m_t}$ in $\tilde{C}_k^{t\,eff}$.

The importance of including the two-loop matching conditions is clearly seen: the dependence on μ_0 decreases from $\pm 16\%$ to around $\pm 2.5\%$ at the representative point $\hat{s} = 0.2$. Most of the effect is due to the strong m_t -dependence of A_{10}^t and to the μ_0 -dependence of $m_t^{\overline{MS}}(\mu_0)$.

In fig. 3, the scale μ_0 is fixed to 120 GeV in $\tilde{C}_k^{t\,eff}$ and to 80 GeV in $\tilde{C}_k^{c\,eff}$, while the scale μ_b takes the values of 2.5, 5 and 10 GeV. One can see that the μ_b -dependence increases after taking into account the $\mathcal{O}(\alpha_s)$ contributions to the effective coefficients. When the $\mathcal{O}(\alpha_s)$ terms are not included, an accidental cancellation of the μ_b -dependence occurs among the four contributions to the differential decay rate in eq. (28). This cancellation becomes exact at $\hat{s} \simeq 0.06$. The $\mathcal{O}(\alpha_s)$ term that plays the major role in changing the μ_b -dependence of A_9^c (see table 4) and in removing this cancellation is proportional to the product of $C_1^{c(1)}(\mu_0) = -15 - 6L$ from the matching conditions and $\ln m_b/\mu_b$ from the one-loop matrix element of P_1^c . A future calculation of the two-loop $b \rightarrow sl^+l^-$ matrix elements of the four-quark operators is desirable, because it should significantly reduce the μ_b -dependence of the prediction for $R_{quark}^{l^+l^-}(\hat{s})$.

When the results described by the solid lines in fig. 3 are integrated over \hat{s} , we obtain

$$\int_{0.05}^{0.25} d\hat{s} R_{quark}^{l^+l^-}(\hat{s}) = (1.36 \pm 0.18) \times 10^{-5}, \quad (49)$$

where only the error from μ_b -dependence is taken into account. Varying $U_{92}^{c(2)}$ from -10 to 10 (as promised at the end of the previous section) would increase the uncertainty by only 0.03 . Thus, calculating the three-loop anomalous dimensions in the future is not expected to have an important impact on the numerical prediction.

In the end, we relate the integrand of $R_{quark}^{l^+l^-}(\hat{s})$ to the physically measurable quantity

$$\begin{aligned} BR[B \rightarrow X_s l^+ l^-]_{\hat{s} \in [0.05, 0.25]} &= BR[B \rightarrow X_c e \bar{\nu}] \int_{0.05}^{0.25} d\hat{s} \left[R_{quark}^{l^+l^-}(\hat{s}) + \delta_{1/m_c^2} R(\hat{s}) + \delta_{1/m_b^2} R(\hat{s}) \right] \\ &= 0.104 [(1.36 \pm 0.18) - 0.02 + 0.06] \times 10^{-5} = (1.46 \pm 0.19) \times 10^{-6}, \end{aligned} \quad (50)$$

where, again, only the error from the μ_b -dependence of $R_{quark}^{l^+l^-}(\hat{s})$ is included. The non-perturbative HQET corrections $\delta_{1/m_c^2} R(\hat{s})$ and $\delta_{1/m_b^2} R(\hat{s})$ have been found with the help of eq. (32) in ref. [5] and eq. (18) in ref. [6], respectively. The $\mathcal{O}(1/m_b^3)$ effects are completely

negligible for $\hat{s} < 0.25$ [19]. The experimental value of 0.104 for the semileptonic branching ratio is taken from ref. [15].

It is worth indicating that additional non-perturbative corrections due to the motion of the b -quark inside the B-meson would occur if we wanted to impose additional cuts on the emitted lepton energies [20]. Such corrections are absent only when the kinematical cut is imposed on nothing but the invariant mass of the lepton pair.

Of course, translating the restriction $\hat{s} \in [0.05, 0.25]$ to bounds in GeV on the lepton invariant mass introduces an additional uncertainty due to the numerical value of $m_{b,pole}$. Since the \hat{s} -spectrum is almost flat in the considered domain, this additional uncertainty (in per cent) will be close to $\frac{5}{4}\sigma_{m_{b,pole}}/m_{b,pole}$, i.e. rather small.

Finally let us note that restricting the studied domain of \hat{s} to $[0.05, 0.25]$ makes the integrated $B \rightarrow X_s l^+ l^-$ branching ratio smaller, but at the same time more sensitive to the sign of $\tilde{C}_7^{eff}(\mu_b)$, when compared to the so-called “non-resonant BR” considered for instance in ref. [21]. If we changed the sign of $\tilde{C}_7^{eff}(\mu_b)$, the last result in eq. (50) would change to 2.92×10^{-6} . Thus, extensions of the SM that predict opposite sign of $\tilde{C}_7^{eff}(\mu_b)$ (like the MSSM in certain dark-matter-favoured regions of its parameter space) might be tested with the help of the integrated BR itself, without considering forward–backward or energy asymmetries.

At this point, we finish our phenomenological discussion, and proceed to describing technical details of the two-loop matching computation in the next section.

5 Two-loop matching for photonic $\Delta B = -\Delta S = 1$ penguins in the Standard Model

5.1. Preliminaries

For processes taking place at energy scales much lower than M_W , the Standard Model can be replaced by an effective theory built out of only light SM fields, i.e. the ones that are much lighter than the W-boson. Our goal here is to find two-loop QCD contributions to the Wilson coefficients of certain operators in the effective theory. The operators we are interested in are the ones giving leading electroweak contributions to the $\Delta B = -\Delta S = 1$ transitions accompanied by either a real photon or a lepton pair emission. In the latter case,

we restrict ourselves to processes mediated by a virtual photon, i.e. we do not consider in this section the SM diagrams where the W or Z boson couple directly to the lepton line.

The simplest way to find the Wilson coefficients is to require equality of the off-shell 1PI amputated Green functions calculated in the full SM and in the effective theory. Up to one loop, we need to consider the $b \rightarrow s\gamma$, $b \rightarrow s$ gluon and $b \rightarrow sc\bar{c}$ functions. At two loops, only the $b \rightarrow s\gamma$ function is necessary. In the cases of $b \rightarrow s\gamma$ and $b \rightarrow s$ gluon, we work at the leading order in α_{em} and up to $\mathcal{O}[(\text{external momenta})^2/M_W^2]$. In the $b \rightarrow sc\bar{c}$ case, external momenta can be neglected.

We set all the light particle masses to zero in the whole calculation. An exception is the b -quark mass, which is being included up to linear order. This means that we maintain m_b only in Yukawa couplings and in the b -quark propagator numerators. The terms of order m_b^2 are neglected. One can justify this procedure by formally treating the b -quark mass term as an interaction with an external scalar field.

In addition, all the Feynman integrands are expanded in external momenta before performing loop integration. Such an expansion, as well as setting all the light masses to zero, creates spurious infrared divergences that we regularize dimensionally. As we shall see, all these divergences cancel out in the matching conditions relating the full and the effective theory Green functions.

The Feynman integrands for the one- and two-loop Feynman diagrams are generated with the help of the program *FeynArts* [22]. After Taylor expansion in external momenta and factorizing them out, the integrals remain dependent only on loop momenta and two heavy masses: M_W and m_t . Subsequent application of the partial fraction decomposition

$$\frac{1}{(q^2 - m_1^2)(q^2 - m_2^2)} = \frac{1}{m_1^2 - m_2^2} \left[\frac{1}{q^2 - m_1^2} - \frac{1}{q^2 - m_2^2} \right] \quad (51)$$

allows a reduction of all the integrals to those in which a single mass parameter occurs in the propagator denominators together with a given loop momentum. Finally, after reduction of tensor integrals to scalar ones, the non-vanishing integrals obtained at one and two loops are respectively as follows:

$$C_n^{(1)} = \frac{(m^2)^{n-2+\epsilon}}{\pi^{2-\epsilon} \Gamma(1+\epsilon)} \int \frac{d^{4-2\epsilon} q}{(q^2 - m^2)^n}, \quad (52)$$

$$C_{n_1 n_2 n_3}^{(2)} = \frac{(m_1^2)^{n_1+n_2+n_3-4+2\epsilon}}{\pi^{4-2\epsilon} \Gamma(1+\epsilon)^2} \int \frac{d^{4-2\epsilon} q_1 d^{4-2\epsilon} q_2}{(q_1^2 - m_1^2)^{n_1} (q_2^2 - m_2^2)^{n_2} [(q_1 - q_2)^2]^{n_3}}, \quad (53)$$

with arbitrary integer powers n , n_1 , n_2 and n_3 , and with m , $m_1 \neq 0$. The chosen normalization makes the results free of trivial common factors.

In eq. (53) we have already made use of the fact that our two-loop scalar integrals always have at least one massless term in their denominators. This turns out to be true in all the Feynman diagrams we have to consider, provided all the light particle masses are set to zero. Therefore, all our two-loop integrals are relatively simple.

The result for the one-loop scalar integral is

$$C_n^{(1)} = i \frac{(-1)^n}{(n-1)!} (1+\epsilon)_{n-3}, \quad (54)$$

which vanishes for $n \leq 0$. Here, $(a)_k$ denotes the Pochhammer symbol equal to

$$(a)_k = \frac{\Gamma(a+k)}{\Gamma(a)} = \begin{cases} a(a+1)(a+2)\dots(a+k-1), & k \geq 1, \\ 1, & k = 0, \\ 1/[(a-1)(a-2)\dots(a-|k|)], & k \leq -1, \end{cases} \quad (55)$$

for integer k and complex a .

The two-loop integrals can easily be found with the help of Feynman parametrization in the cases when $m_1 = m_2$ or $m_2 = 0$

$$C_{n_1 n_2 n_3}^{(2)} \Big|_{m_1=m_2} = (-1)^{n_1+n_2+n_3+1} \frac{(2-\epsilon)_{-n_3} (1+\epsilon)_{n_1+n_3-3} (1+\epsilon)_{n_2+n_3-3}}{(n_1-1)!(n_2-1)!(n_1+n_2+n_3-4+2\epsilon)_{n_3}}, \quad (56)$$

$$C_{n_1 n_2 n_3}^{(2)} \Big|_{m_2=0} = (-1)^{n_1+n_2+n_3+1} \frac{(1+2\epsilon)_{n_1+n_2+n_3-5} (1+\epsilon)_{n_2+n_3-3} (1-\epsilon)_{1-n_2} (1-\epsilon)_{1-n_3}}{(n_1-1)!(n_2-1)!(n_3-1)!(1-\epsilon)(1-\frac{1}{3}\pi^2\epsilon^2 + \mathcal{O}(\epsilon^3))}. \quad (57)$$

It remains to discuss the case when $m_1 \neq m_2$ and none of the two masses vanishes. The starting point is the integral $C_{111}^{(2)}$, which equals:

$$C_{111}^{(2)} = \frac{1}{2(1-\epsilon)(1-2\epsilon)} \left[-\frac{1+x}{\epsilon^2} + \frac{2}{\epsilon} x \ln x + (1-2x) \ln^2 x + 2(1-x) Li_2 \left(1 - \frac{1}{x} \right) + \mathcal{O}(\epsilon) \right], \quad (58)$$

where $x = m_2^2/m_1^2$ [23]. All the integrals with three positive indices can be derived from the above result with the help of the following recurrence relations [23]:

$$\begin{aligned} C_{(n_1+1)n_2n_3}^{(2)} &= \frac{1}{n_1(1-x)} \left\{ [4-2\epsilon-n_1-n_2-n_3+x(n_1-n_3)] C_{n_1n_2n_3}^{(2)} \right. \\ &\quad \left. + x n_2 [C_{(n_1-1)(n_2+1)n_3}^{(2)} - C_{n_1(n_2+1)(n_3-1)}^{(2)}] \right\}, \\ C_{n_1(n_2+1)n_3}^{(2)} &= -\frac{1}{n_2x(1-x)} \left\{ [x(4-2\epsilon-n_1-n_2-n_3) + n_2 - n_3] C_{n_1n_2n_3}^{(2)} \right. \\ &\quad \left. + n_1 [C_{(n_1+1)(n_2-1)n_3}^{(2)} - C_{(n_1+1)n_2(n_3-1)}^{(2)}] \right\}, \quad (59) \\ C_{n_1n_2(n_3+1)}^{(2)} &= \frac{1}{n_3(1-x)^2} \left\{ [(1+x)(-4+2\epsilon) + 2n_2 + (1+3x)n_3] C_{n_1n_2n_3}^{(2)} \right. \\ &\quad \left. + 2x n_2 [C_{n_1(n_2+1)(n_3-1)}^{(2)} - C_{(n_1-1)(n_2+1)n_3}^{(2)}] \right. \\ &\quad \left. + (1-x)n_3 [C_{n_1(n_2-1)(n_3+1)}^{(2)} - C_{(n_1-1)n_2(n_3+1)}^{(2)}] \right\}. \end{aligned}$$

All the two-loop integrals defined in eq. (53) vanish when either n_1 or n_2 is non-positive. When these two indices are positive but n_3 is non-positive, they reduce to products of one-loop tensor integrals. It is sensible to make this reduction only in the case when the two masses are different and non-vanishing. Then we obtain

$$C_{n_1 n_2 n_3}^{(2)} \stackrel{n_3 \leq 0}{=} \sum_{k=0}^{\lfloor \frac{-n_3}{2} \rfloor} \sum_{j=0}^{-n_3-2k} \binom{-n_3}{2k} \binom{-n_3-2k}{j} \frac{x^{2-n_2+k+j-\epsilon} (-1)^{n_1+n_2+n_3+1} (2k)!}{(n_1-1)! (n_2-1)! k! (2-\epsilon)_k} \times \\ \times (2-\epsilon)_{j+k} (2-\epsilon)_{-n_3-k-j} (1+\epsilon)_{n_2-k-j-3} (1+\epsilon)_{n_1+n_3+k+j-3}. \quad (60)$$

Otherwise, one can use eqs. (56) and (57), which apply for non-positive n_3 , too. Equation (57) gives zero in such a case, but eq. (56) does not.

5.2. The Standard Model side

Let us start with calculating the $b \rightarrow s\gamma$ function up to two loops. There is no tree-level contribution to this function in the Standard Model. The four 1PI diagrams arising at one loop are presented in fig. 4.

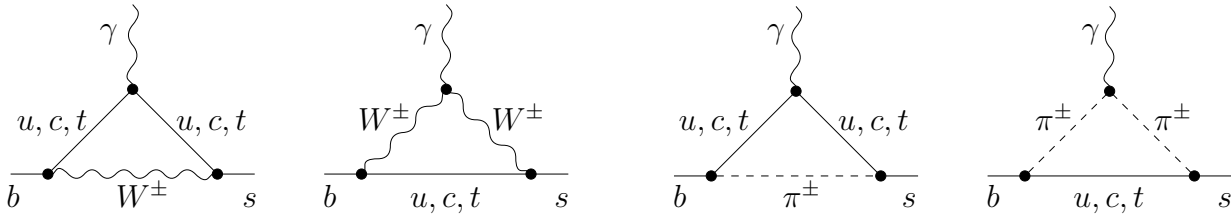


Figure 4: One-loop 1PI diagrams for $b \rightarrow s\gamma$ in the SM. The charged would-be Goldstone boson is denoted by π^\pm . There is no $W^\pm \pi^\mp \gamma$ coupling in the background-field gauge.

We calculate the corresponding unrenormalized amputated Green function off shell, in the background-field version of the 't Hooft-Feynman gauge. The Feynman integrands are expanded up to the second order in external momenta and m_b (neglecting m_b^2 though). As in section 2, we refrain from using unitarity of the CKM matrix here. The result can be written in the following form:

$$i \frac{4G_F}{\sqrt{2}} \frac{eP_R}{(4\pi)^2} N_\epsilon^{(1)} \left\{ (V_{us}^* V_{ub} + V_{cs}^* V_{cb}) \sum_{j=1}^{13} h_j^{(1)} S_j + V_{ts}^* V_{tb} \sum_{j=1}^{13} f_j^{(1)}(x) S_j \right\} + \mathcal{O}(\epsilon^2), \quad (61)$$

where $P_R = \frac{1}{2}(1 + \gamma_5)$, $N_\epsilon^{(1)} = 1 - \epsilon\kappa + \epsilon^2(\frac{1}{12}\pi^2 + \frac{1}{2}\kappa^2)$, $\kappa = \gamma_E - \ln(4\pi) + \ln(M_W^2/\mu_0^2)$ and S_k stand for Dirac structures that depend on the incoming b -quark momentum p and on the

outgoing photon momentum k

$$S_j = \left(\gamma_\mu \not{p} \not{k}, \gamma_\mu (p \cdot k), \gamma_\mu p^2, \gamma_\mu k^2, \not{p} k_\mu, \not{p} p_\mu, \not{k} p_\mu, \not{k} k_\mu, \right. \\ \left. m_b \not{k} \gamma_\mu, m_b \gamma_\mu \not{k}, m_b \not{p} \gamma_\mu, m_b \gamma_\mu \not{p}, M_W^2 \gamma_\mu \right)_j. \quad (62)$$

As we shall see later, explicit results are needed only for the coefficients at the structures S_2 , S_8 and S_{10} . We find

$$h_2^{(1)} = \frac{23}{9} + \frac{145}{54} \epsilon, \quad h_8^{(1)} = -\frac{4}{9\epsilon} + \frac{7}{54} + \frac{59}{324} \epsilon, \quad h_{10}^{(1)} = 0, \\ f_2^{(1)}(x) = \frac{15x^3 - 16x^2 + 4x}{3(x-1)^4} \ln x + \frac{-8x^3 - 105x^2 + 141x - 46}{18(x-1)^3} \\ + \epsilon \left\{ \frac{-15x^3 + 16x^2 - 4x}{6(x-1)^4} \ln^2 x + \frac{8x^4 + 115x^3 - 150x^2 + 48x}{18(x-1)^4} \ln x + \frac{-76x^3 - 645x^2 + 885x - 290}{108(x-1)^3} \right\}, \\ f_8^{(1)}(x) = \frac{-3x^4 - 15x^3 - 6x^2 + 20x - 8}{18(x-1)^4} \ln x + \frac{71x^3 + 78x^2 - 111x + 34}{108(x-1)^3} + \epsilon \left\{ \frac{3x^4 + 15x^3 + 6x^2 - 20x + 8}{36(x-1)^4} \ln^2 x \right. \\ \left. + \frac{-71x^4 - 79x^3 + 162x^2 - 144x + 48}{108(x-1)^4} \ln x + \frac{529x^3 - 102x^2 + 195x - 118}{648(x-1)^3} \right\}, \\ f_{10}^{(1)}(x) = \frac{-3x^2 + 2x}{6(x-1)^3} \ln x + \frac{5x^2 - 3x}{12(1-x)^2} + \epsilon \left\{ \frac{3x^2 - 2x}{12(x-1)^3} \ln^2 x + \frac{-5x^3 + 2x^2}{12(x-1)^3} \ln x + \frac{11x^2 - 5x}{24(x-1)^2} \right\}, \quad (63)$$

where $x = m_t^2/M_W^2$.

Let us now proceed to an evaluation of the first QCD correction to the considered Green function. The corresponding two-loop diagrams are shown in fig. 5.

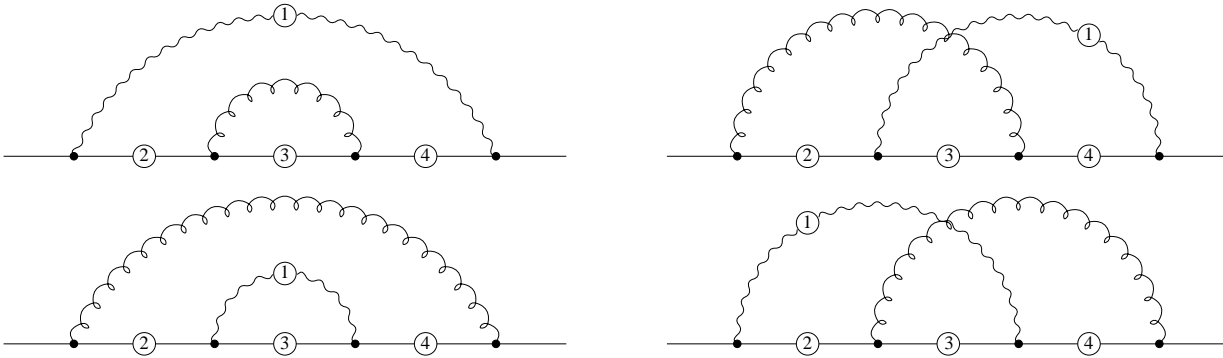


Figure 5: Two-loop 1PI diagrams for $b \rightarrow s\gamma$ in the SM. The wavy lines denote either the W -boson or the charged would-be Goldstone boson. The external photon can couple at any of the places marked by small circles.

In analogy to eq. (61), we write the unrenormalized two-loop result as

$$i \frac{4G_F}{\sqrt{2}} \frac{eg^2 P_R}{(4\pi)^4} N_\epsilon^{(2)} \left\{ (V_{us}^* V_{ub} + V_{cs}^* V_{cb}) \sum_{j=1}^{13} h_j^{(2)} S_j + V_{ts}^* V_{tb} \sum_{j=1}^{13} f_j^{(2)}(x) S_j \right\} + \mathcal{O}(\epsilon), \quad (64)$$

where g is the QCD gauge coupling and $N_\epsilon^{(2)} = 1 - 2\epsilon\kappa + \epsilon^2(\frac{1}{6}\pi^2 + 2\kappa^2)$. The two-loop analogues of the coefficients given in eq. (63) are found to have the following form:

$$\begin{aligned}
h_2^{(2)} &= -\frac{272}{81\epsilon} - \frac{3740}{243}, & h_8^{(2)} &= -\frac{128}{81\epsilon^2} - \frac{1088}{243\epsilon} - \frac{314}{729} - \frac{128\pi^2}{243}, & h_{10}^{(2)} &= \frac{20}{9\epsilon} + \frac{92}{27}, \\
f_2^{(2)}(x) &= \frac{1}{\epsilon} \left\{ \frac{8x(-45x^3-34x^2+53x-10)}{9(x-1)^5} \ln x + \frac{4(x^4+641x^3-501x^2+83x-8)}{27(x-1)^4} \right\} \\
&+ \frac{8x(7x^3-69x^2+61x-14)}{9(x-1)^4} Li_2\left(1 - \frac{1}{x}\right) + \frac{4x(45x^3+34x^2-53x+10)}{3(x-1)^5} \ln^2 x \\
&+ \frac{4(-6x^5-4497x^4+2622x^3+811x^2-638x+88)}{81(x-1)^5} \ln x + \frac{2(-719x^4+35822x^3-35073x^2+11492x-1802)}{243(x-1)^4}, \\
f_8^{(2)}(x) &= \frac{1}{\epsilon} \left\{ \frac{4(243x^4+486x^3-419x^2+130x-8)}{81(x-1)^5} \ln x + \frac{2(-185x^4-3313x^3+369x^2+905x-368)}{243(x-1)^4} \right\} \\
&+ \frac{4(32x^4+283x^3-135x^2-70x+64)}{81(x-1)^4} Li_2\left(1 - \frac{1}{x}\right) + \frac{2(-243x^4-486x^3+419x^2-130x+8)}{27(x-1)^5} \ln^2 x \\
&+ \frac{2(370x^5+7933x^4-1370x^3-683x^2+238x-8)}{243(x-1)^5} \ln x + \frac{2(-3301x^4-20714x^3+4182x^2+202x+191)}{729(x-1)^4}, \\
f_{10}^{(2)}(x) &= \frac{1}{\epsilon} \left\{ \frac{2x(36x^2+x-10)}{9(x-1)^4} \ln x + \frac{11x^3-169x^2+132x-28}{9(x-1)^3} \right\} + \frac{2x(-15x^3+8x^2-21x+10)}{9(x-1)^4} Li_2\left(1 - \frac{1}{x}\right) \\
&+ \frac{x(-36x^2-x+10)}{3(x-1)^4} \ln^2 x + \frac{-22x^4+396x^3-377x^2+142x-16}{9(x-1)^4} \ln x + \frac{31x^3-1071x^2+630x-112}{54(x-1)^3}.
\end{aligned} \tag{65}$$

The last two elements we need to know on the SM side are the $b \rightarrow s$ gluon and $b \rightarrow s\bar{c}$ functions up to one loop. They are used to recover one-loop contributions to certain Wilson coefficients which take part in the two-loop $b \rightarrow s\gamma$ matching condition.

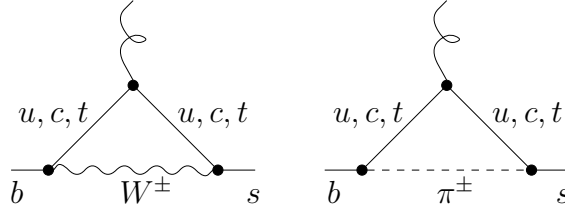


Figure 6: One-loop 1PI diagrams for $b \rightarrow s$ gluon in the SM.

Similarly to the $b \rightarrow s\gamma$ case, there is no tree-level contribution to the $b \rightarrow s$ gluon Green function in the SM. The one-loop contribution is given by the two diagrams presented in fig. 6. In analogy to eq. (61), the result can be written as

$$i \frac{4G_F g P_R T^a}{\sqrt{2} (4\pi)^2} N_\epsilon^{(1)} \left\{ (V_{us}^* V_{ub} + V_{cs}^* V_{cb}) \sum_{j=1}^{13} u_j^{(1)} S_j + V_{ts}^* V_{tb} \sum_{j=1}^{13} v_j^{(1)}(x) S_j \right\} + \mathcal{O}(\epsilon^2), \tag{66}$$

where T^a denotes the SU(3) generator corresponding to the outgoing gluon. The coefficients at the structures S_2 , S_8 and S_{10} read

$$u_2^{(1)} = \frac{4}{3} + \frac{22}{9}\epsilon, \quad u_8^{(1)} = -\frac{2}{3\epsilon} + \frac{1}{9} + \frac{11}{54}\epsilon, \quad u_{10}^{(1)} = 0, \tag{67}$$

$$\begin{aligned}
v_2^{(1)}(x) &= \frac{-5x^2+2x}{(x-1)^4} \ln x + \frac{-x^3+15x^2+12x-8}{6(x-1)^3} \\
&+ \epsilon \left\{ \frac{5x^2-2x}{2(x-1)^4} \ln^2 x + \frac{x^4-16x^3-30x^2+24x}{6(x-1)^4} \ln x + \frac{-5x^3+159x^2+60x-88}{36(x-1)^3} \right\}, \\
v_8^{(1)}(x) &= \frac{3x^2+5x-2}{3(x-1)^4} \ln x + \frac{5x^3-12x^2-39x+10}{18(x-1)^3} \\
&+ \epsilon \left\{ \frac{-3x^2-5x+2}{6(x-1)^4} \ln^2 x + \frac{-5x^4+17x^3+54x^2-36x+12}{18(x-1)^4} \ln x + \frac{19x^3-192x^2-57x-22}{108(x-1)^3} \right\}, \\
v_{10}^{(1)}(x) &= \frac{x}{2(x-1)^3} \ln x + \frac{x^2-3x}{4(x-1)^2} + \epsilon \left\{ \frac{-x}{4(x-1)^3} \ln^2 x + \frac{-x^3+4x^2}{4(x-1)^3} \ln x + \frac{x^2-7x}{8(x-1)^2} \right\}.
\end{aligned} \tag{68}$$

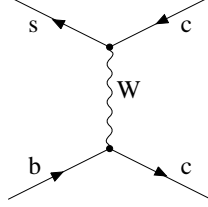


Figure 7: Tree-level $b \rightarrow sc\bar{c}$ diagram on the SM side.

Contrary to the functions considered so far, the $b \rightarrow sc\bar{c}$ function does acquire a tree-level contribution in the SM. It is given by the diagram shown in fig. 7. For vanishing external momenta, it gives⁸

$$-i \frac{4G_F}{\sqrt{2}} V_{cs}^* V_{cb} (\gamma_\mu P_L) \otimes (\gamma^\mu P_L). \tag{69}$$

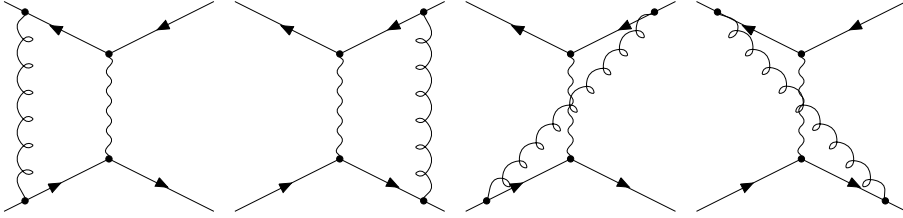


Figure 8: One-loop $b \rightarrow sc\bar{c}$ diagrams on the SM side, which do not vanish in dimensional regularization when all the light particle masses are set to zero.

The non-vanishing one-loop diagrams for the $b \rightarrow sc\bar{c}$ functions are shown in fig. 8. When the external momenta are set to zero, we find the following result for the corresponding amputated Green function:

$$i \frac{4G_F}{\sqrt{2}} \frac{g^2}{(4\pi)^2} V_{cs}^* V_{cb} N_\epsilon^{(1)} \left\{ \left(-\frac{6}{\epsilon} - 15 - \frac{39}{2}\epsilon \right) (\gamma_\mu P_L T^a) \otimes (\gamma^\mu P_L T^a) + \left(-\frac{1}{\epsilon} - \frac{3}{2} + \mathcal{O}(\epsilon) \right) \times \right.$$

⁸ The tensor product symbol $\Gamma \otimes \Gamma'$ is used here to denote the tree-level $(s\bar{\Gamma}c)(\bar{c}\Gamma'b)$ amputated Green function.

$$\times [(\gamma_\mu \gamma_\nu \gamma_\rho P_L T^a) \otimes (\gamma^\mu \gamma^\nu \gamma^\rho P_L T^a) - 16(\gamma_\mu P_L T^a) \otimes (\gamma^\mu P_L T^a)] + \mathcal{O}(\epsilon^2). \quad (70)$$

The Dirac structure in the last line of the above equation vanishes in four dimensions. However, there is no way to express it as $\epsilon \times (\text{simpler structure})$. The coefficient at this structure will give us the Wilson coefficient of an evanescent operator in the effective theory [24]. The necessity of recovering this coefficient (as well as keeping $\mathcal{O}(\epsilon)$ parts of other one-loop coefficients) is a price we have to pay for regularizing infrared divergences dimensionally.

The above result is the last one we need to know on the SM side. In the next subsection, we shall study the same Green functions in the effective theory framework.

5.3. The effective theory side

The lagrangian of the effective theory has been given in eq. (1). At present, we need to include in addition several non-physical operators. We write

$$\begin{aligned} \mathcal{L}_{eff} = & \mathcal{L}_{QCD \times QED}(u, d, s, c, b, e, \mu, \tau) + \frac{4G_F}{\sqrt{2}} \left\{ \sum_{Q=u,c} V_{Qs}^* V_{Qb} (C_1^c P_1^Q + C_2^c P_2^Q + C_{11}^c P_{11}^Q) \right. \\ & \left. + \sum_i [(V_{us}^* V_{ub} + V_{cs}^* V_{cb}) C_i^c + V_{ts}^* V_{tb} C_i^t] P_i \right\}. \end{aligned} \quad (71)$$

The operators P_i^Q and P_i entering the effective lagrangian can be divided into three classes: physical, evanescent (i.e. algebraically vanishing in four dimensions) and EOM-vanishing (i.e. vanishing by the QCD \times QED equations of motion, up to a total derivative).

The physical operators have already been given in eq. (2). However, for the purpose of the present section, it is convenient to redefine P_9 so that it contains a sum over all the light charged fermions f weighted by their electric charges Q_f

$$P_9 = -\frac{e^2}{g^2} (\bar{s}_L \gamma_\mu b_L) \sum_f Q_f (\bar{f} \gamma^\mu f). \quad (72)$$

Such a redefinition of P_9 does not alter its Wilson coefficient at leading order in electroweak interactions.

As far as the evanescent operators are concerned, only P_{11}^Q from the appendix will be needed in the present section.

The gauge-invariant EOM-vanishing operators can be chosen as

$$P_{31} = \frac{1}{g} (\bar{s}_L \gamma^\mu T^a b_L) D^\nu G_{\mu\nu}^a + P_4,$$

$$\begin{aligned}
P_{32} &= \frac{1}{g^2} m_b \bar{s}_L \not{D} \not{D} b_R, \\
P_{33} &= \frac{i}{g^2} \bar{s}_L \not{D} \not{D} \not{D} b_L, \\
P_{34} &= \frac{i}{g} \left[\bar{s}_L \overleftarrow{\not{D}} \sigma^{\mu\nu} T^a b_L G_{\mu\nu}^a - G_{\mu\nu}^a \bar{s}_L T^a \sigma^{\mu\nu} \not{D} b_L \right] + P_8, \\
P_{35} &= \frac{ie}{g^2} \left[\bar{s}_L \overleftarrow{\not{D}} \sigma^{\mu\nu} b_L F_{\mu\nu} - F_{\mu\nu} \bar{s}_L \sigma^{\mu\nu} \not{D} b_L \right] + P_7, \\
P_{36} &= \frac{e}{g^2} (\bar{s}_L \gamma^\mu b_L) \partial^\nu F_{\mu\nu} - P_9.
\end{aligned} \tag{73}$$

Our sign convention in the covariant derivative acting on a quark field ψ is

$$D_\mu \psi = \left(\partial_\mu + ig G_\mu^a T^a + ie Q_\psi A_\mu \right) \psi. \tag{74}$$

The EOM-vanishing operators in eq. (73) can be assumed to contain the background gluon field only, because nothing but their tree-level matrix elements will be needed for the off-shell matching in the next subsection. However, a systematic off-shell renormalization of the effective theory requires introducing EOM-vanishing operators that contain the quantum gluon field as well. The explicit form of such operators is irrelevant here. Nevertheless, one should not forget that all of them enter into the sums over operators, such as the one in the last term of eq. (71).

It is not completely trivial to convince oneself that eq. (73) indeed contains all the gauge-invariant EOM-vanishing operators that we may encounter. One way to do this is to first write all the $\Delta B = -\Delta S = 1$ operators of dimension 5 and 6 containing the left-handed s -quark field only.⁹ The derivatives acting on the s -quark field can be removed by parts. One can start from writing down the 6 possible operators that contain the chromomagnetic and electromagnetic field strength tensors or their duals

$$\begin{aligned}
(\bar{s}_L T^a \sigma^{\mu\nu} b_R) G_{\mu\nu}^a, & \quad (\bar{s}_L T^a \gamma^\mu b_L) D^\nu G_{\mu\nu}^a, & \quad (\bar{s}_L T^a \gamma^\mu D^\nu b_L) \tilde{G}_{\mu\nu}^a, \\
(\bar{s}_L \sigma^{\mu\nu} b_R) F_{\mu\nu}, & \quad (\bar{s}_L \gamma^\mu b_L) \partial^\nu F_{\mu\nu}, & \quad (\bar{s}_L \gamma^\mu D^\nu b_L) \tilde{F}_{\mu\nu}.
\end{aligned} \tag{75}$$

Nothing new is obtained from the first two pairs of operators above, when the field strength tensors are replaced by their duals, because of the Bianchi identity and $\sigma_{\alpha\beta\gamma\delta} \sim \varepsilon_{\alpha\beta\gamma\delta} \sigma^{\gamma\delta}$. On the other hand, replacing the dual tensors by ordinary ones in the last pair of operators would break CP combined with $b \leftrightarrow s$ interchange even for $m_b = 0$ and real CKM angles.

⁹ Here, the dimension of an operator is understood as the sum of dimensions of the fields and derivatives it contains. Explicit mass factors in the normalization are not counted.

The remaining operators (apart from the four-fermion ones) must contain covariant derivatives. Since commutators of the covariant derivatives give field strength tensors, only one additional operator with three covariant derivatives (e.g. $\bar{s}_L \not{D} D^2 b_L$) and one operator with two covariant derivatives (e.g. $\bar{s}_L D^2 b_L$) remains. At this point, one has at hand a complete set of 8 gauge-invariant operators (apart from the four-fermion ones). The “magnetic moment” operators P_7 , P_8 and the EOM-vanishing operators P_{31} , ..., P_{36} are just certain linear combinations of them, P_4 and P_9 (up to total derivatives).

Since both the u - and c -quarks are treated as massless in the present calculation, the lagrangian is symmetric under $u \leftrightarrow c$ exchange. This symmetry has already been taken into account in eq. (71): the same Wilson coefficients C_i^c occur both in the u -quark and the c -quark sectors.

The lagrangian (71) is written in terms of bare fields and parameters. In order to express it in terms of the QCD-renormalized quantities, we replace

$$g \rightarrow Z_g g, \quad m_b \rightarrow Z_m m_b, \quad \psi \rightarrow Z_\psi^{1/2} \psi, \quad C_i^Q \rightarrow \sum_j C_j^Q Z_{ji}, \quad (76)$$

for the QCD gauge coupling, b -quark mass, quark fields and the Wilson coefficients, respectively. As far as the background gluon field $G_\mu^{(b)}$ is concerned, we only need to remember that $gG_\mu^{(b)}$ does not get renormalized.

After QCD renormalization, the structure of the effective lagrangian is the same as in eq. (71), but the Wilson coefficients C_i^Q are replaced by some other constants that we denote here by A_i^Q . Below, we shall need

$$\begin{aligned} A_j^Q &= Z_\psi^2 \sum_i C_i^Q Z_{ij} && \text{for } j = 1, 2, 4, 11, \\ A_7^Q &= Z_\psi Z_g^{-2} \left[Z_m \sum_i C_i^Q Z_{i7} + (Z_m - 1) \sum_i C_i^Q Z_{i(35)} \right], \\ A_8^Q &= Z_\psi Z_g^{-2} \left[Z_m \sum_i C_i^Q Z_{i8} + (Z_m - 1) \sum_i C_i^Q Z_{i(34)} \right], \\ A_9^Q &= Z_\psi Z_g^{-2} \sum_i C_i^Q Z_{i9}. \end{aligned} \quad (77)$$

For simplicity, we shall use the \overline{MS} scheme in the present section. The \overline{MS} results for the Wilson coefficients will be obtained later from the MS ones by simply setting $\gamma_E - \ln(4\pi)$ to zero, i.e. replacing κ by $\ln(M_W^2/\mu_0^2)$.

In the MS scheme, the renormalization constants read

$$\begin{aligned}
Z_g &= 1 + \frac{g^2}{(4\pi)^2\epsilon} \left(-\frac{1}{2}\beta_0\right) + \mathcal{O}(g^4) && \text{with } \beta_0 = \frac{23}{3} \text{ for 5 active flavours,} \\
Z_m &= 1 + \frac{g^2}{(4\pi)^2\epsilon} \left(-\frac{1}{2}\gamma_m^{(0)}\right) + \mathcal{O}(g^4) && \text{with } \gamma_m^{(0)} = 8, \\
Z_\psi &= 1 + \frac{g^2}{(4\pi)^2\epsilon} \left(-\gamma_\psi^{(0)}\right) + \mathcal{O}(g^4) && \text{with } \gamma_\psi^{(0)} = \frac{4}{3}, \\
Z_{ij} &= \delta_{ij} + \frac{g^2}{(4\pi)^2} \left[a_{ij}^{01} + \frac{1}{\epsilon} a_{ij}^{11} \right] + \frac{g^4}{(4\pi)^4} \left[a_{ij}^{02} + \frac{1}{\epsilon} a_{ij}^{12} + \frac{1}{\epsilon^2} a_{ij}^{22} \right] + \mathcal{O}(g^6). \tag{78}
\end{aligned}$$

The finite terms a_{ij}^{0k} can be different from zero if and only if P_i is an evanescent operator and P_j is not. Values of a_{ij}^{0k} are fixed by requiring that renormalized matrix elements of evanescent operators vanish in 4 dimensions [24]. This requirement is just an extension of the *MS*-scheme definition to situations where evanescent operators are present.

Our off-shell operator basis is chosen in such a manner that as many operators as possible are EOM-vanishing. This means that no linear combination of the remaining operators is EOM-vanishing. In such a case, the EOM-vanishing operators do not mix into the remaining ones, i.e. $Z_{ij} = 0$ when P_i is EOM-vanishing and P_j is not. In consequence, we shall need to know explicitly only the mixing among the physical and evanescent operators.¹⁰

The powers of coupling constants in front of our operators have been chosen in such a way that terms of order g^{2n} in the renormalization constants originate from n-loop diagrams in the effective theory. As one can see, the sum of powers of gauge coupling constants in front of a given operator is always equal to “(number of fields in this operator)–4”. In the original QCD and QED lagrangians, the powers of coupling constants are equal to “(number of fields)–2”. Here, two powers are traded for G_F that normalizes the effective lagrangian.

The renormalization constants are found by calculating ultraviolet divergent parts of Feynman diagrams in the effective theory. When doing this, it is essential to clearly separate ultraviolet and infrared divergences. In order to do so, one can introduce an auxiliary mass parameter into all the propagator denominators (including the gluon ones), as explained in ref. [25]. All the renormalization constants in the effective theory up to two loops are known from the former anomalous dimension computations [7, 8, 9, 14] (although some of them need to be transformed to the “new” operator basis (2)). Here, we shall need the one-loop

¹⁰ Getting rid of $Z_{i(34)}$ and $Z_{i(35)}$, which enter eq. (77), is somewhat tricky – see subsection 5.4.

renormalization constant matrix \hat{a}^{11} for $\{P_1, P_2, P_4, P_7, P_8, P_9, P_{11}\}$ only. It reads

$$\hat{a}^{11} = \begin{bmatrix} * & * & * & 0 & 0 & -\frac{16}{27} & * \\ 6 & 0 & \frac{2}{3} & 0 & 0 & -\frac{4}{9} & 1 \\ 0 & 0 & * & 0 & 0 & \frac{16}{27} & 0 \\ 0 & 0 & 0 & \frac{16}{3} - \beta_0 & 0 & 0 & 0 \\ 0 & 0 & 0 & -\frac{16}{9} & * & 0 & 0 \\ 0 & 0 & 0 & 0 & 0 & -\beta_0 & 0 \\ 0 & 0 & 0 & 0 & 0 & 0 & * \end{bmatrix}, \quad (79)$$

where stars denote non-vanishing entries that are irrelevant for us.

In addition, for the two-loop matching of photonic penguins in the charm sector, we shall need

$$\begin{aligned} a_{27}^{12} &= \frac{116}{81}, & a_{27}^{22} &= 0, & a_{(11)7}^{01} &= 0, \\ a_{29}^{12} &= \frac{776}{243}, & a_{29}^{22} &= \frac{148}{81}, & a_{(11)9}^{01} &= \frac{64}{27}. \end{aligned} \quad (80)$$

At this point, we are ready to calculate all the necessary 1PI Green functions on the effective theory side. This turns out to be very simple, because all the particles in the effective theory are massless in our approach.¹¹ Consequently, all the loop diagrams vanish in dimensional regularization, because of the cancellation between ultraviolet and infrared divergences. In effect, we need to know only the tree-level matrix element of the effective lagrangian. The ultraviolet counterterms present in this matrix element reproduce precisely the infrared divergences in the effective theory, which have to be equal to the infrared divergences on the SM side. As we shall see, all the $1/\epsilon^n$ poles will indeed cancel in the matching condition.

External gluons in the Green functions considered on the Standard Model side have been the background ones. Therefore, we can maintain only the background gluon field in \mathcal{L}_{eff} , since only tree-level diagrams are non-vanishing on the effective theory side. This is why we could omit EOM-vanishing operators proportional to quantum gluons in our operator basis, even though the calculation is performed off-shell.

We now write down the effective theory counterparts of the Green functions considered in subsection 5.2. Their structure follows directly from tree-level Feynman rules for the operators given in eqs. (2) and (73).

¹¹ Remember that the b -quark mass is formally treated here as a perturbative interaction with an external scalar field, and we include only terms that are linear in this interaction.

The $b \rightarrow s\gamma$ function reads (cf. eq. (61))

$$i\frac{4G_F}{\sqrt{2}}\frac{eP_R}{g^2}\left\{(V_{us}^*V_{ub}+V_{cs}^*V_{cb})\sum_{j=1}^{12}\tilde{h}_jS_j+V_{ts}^*V_{tb}\sum_{j=1}^{12}\tilde{f}_jS_j\right\}\quad (81)$$

with the coefficients at the structures S_2 , S_8 and S_{10} given by

$$\begin{aligned}\tilde{h}_2 &= -4A_{35}^c, & \tilde{h}_8 &= 2A_{35}^c - A_{36}^c, & \tilde{h}_{10} &= A_7^c + A_{35}^c, \\ \tilde{f}_2 &= -4A_{35}^t, & \tilde{f}_8 &= 2A_{35}^t - A_{36}^t, & \tilde{f}_{10} &= A_7^t + A_{35}^t.\end{aligned}\quad (82)$$

to all orders in QCD. Similarly, for $b \rightarrow s$ gluon we get

$$i\frac{4G_F}{\sqrt{2}}\frac{P_RT^a}{g}\left\{(V_{us}^*V_{ub}+V_{cs}^*V_{cb})\sum_{j=1}^{12}\tilde{u}_jS_j+V_{ts}^*V_{tb}\sum_{j=1}^{12}\tilde{v}_jS_j\right\}\quad (83)$$

with

$$\begin{aligned}\tilde{u}_2 &= -4A_{34}^c, & \tilde{u}_8 &= 2A_{34}^c - A_{31}^c, & \tilde{u}_{10} &= A_8^c + A_{34}^c, \\ \tilde{v}_2 &= -4A_{34}^t, & \tilde{v}_8 &= 2A_{34}^t - A_{31}^t, & \tilde{v}_{10} &= A_8^t + A_{34}^t.\end{aligned}\quad (84)$$

In both the $b \rightarrow s\gamma$ and $b \rightarrow s$ gluon cases, the coefficients at other structures depend on A_{32}^Q and A_{33}^Q , too. In each of these two cases, coefficients at 12 independent Dirac structures S_j are given by linear combinations of only 6 independent quantities. It is just a consequence of QCD×QED gauge invariance of our effective lagrangian. Therefore, the coefficients at the structures S_k must satisfy $12 - 6 = 6$ linear constraints. This must be the case also for the SM Green functions, because they must match the effective theory ones. Checking these constraints on the SM side has been an important cross-check in our calculation.

The last function we have to consider on the effective theory side is the $b \rightarrow sc\bar{c}$ one. It takes the form

$$\begin{aligned}&i\frac{4G_F}{\sqrt{2}}V_{cs}^*V_{cb}\{A_1^c(\gamma_\mu P_L T^a)\otimes(\gamma^\mu P_L T^a)+A_2^c(\gamma_\mu P_L)\otimes(\gamma^\mu P_L) \\ &+A_{11}^c[(\gamma_\mu\gamma_\nu\gamma_\rho P_L T^a)\otimes(\gamma^\mu\gamma^\nu\gamma^\rho P_L T^a)-16(\gamma_\mu P_L T^a)\otimes(\gamma^\mu P_L T^a)]\} \\ &+[\text{terms proportional to } (A_{31}^Q+A_4^Q)].\end{aligned}\quad (85)$$

5.4. The matching

The Wilson coefficients can be perturbatively expanded as in eq. (3). We shall first recover the Wilson coefficients at all the EOM-non-vanishing operators up to one loop. Then, two-loop contributions to the coefficients at P_7 and P_9 will be found.

A careful reader might be surprised that we start the matching without having considered diagrams with UV counterterms on the SM side. Apart from the electroweak counterterm proportional to $\bar{s}\not{D}b$, we should include QCD renormalization of the quark wave functions and masses.

The electroweak counterterm proportional to $\bar{s}\not{D}b$ is taken in the MOM scheme, at $q^2 = 0$ for the $\bar{s}\not{D}b$ term, and at vanishing external momenta for the terms containing gauge bosons. It is achieved by an appropriate flavour-off-diagonal renormalization of the quark wave functions. The only effect of such a renormalization in the present case is that the coefficients at the structure S_{13} in eqs. (61), (64) and (66) are completely renormalized away. This is welcome, because the structure S_{13} was absent from the effective theory counterparts of these equations (eqs. (81) and (83)).

As far as the QCD renormalization of the quark wave functions in internal lines and in vertices is concerned, it combines to an overall factor, which could be obtained by renormalizing only those terms in the vertices that correspond to external fields in a given Green function. However, one-loop external quark field renormalization is the same on the full and effective theory sides. Consequently, we can omit counterterms with Z_ψ on the SM side and simultaneously set Z_ψ to unity on the effective theory side.

The same refers to the renormalization of the b -quark mass, since m_b is actually treated as an external scalar field. We omit the corresponding counterterms on the full theory side and simultaneously set Z_m to unity on the effective theory side. This is how we get rid of terms proportional to $(Z_m - 1)$ in eq. (77).

As far as the renormalization of the QCD gauge coupling is concerned, no such counterterms occur on the full theory side in our particular calculation. On the effective theory side, we maintain all the necessary factors of Z_g .

The last relevant quantity that acquires QCD renormalization on the full theory side is the top quark mass. However, contributions from the corresponding counterterm diagrams can be obtained by differentiating lower order results with respect to m_t (see below).

Let us first match the $b \rightarrow sc\bar{c}$ Green function up to one loop. The first thing to notice is that terms proportional to $A_{31}^Q + A_4^Q$ in the last line of eq. (85) are not important at the considered order, because

$$A_4^Q = -A_{31}^Q + \mathcal{O}(g^4). \quad (86)$$

The reason for this relation is that the $b \rightarrow s d \bar{d}$ 1PI Green function acquires its leading contribution only at two loops in the SM. Lower-order tree-level contributions to this function must vanish in the effective theory, which implies the above relation.

Similarly, from the fact that the $b \rightarrow s e^+ e^-$ 1PI function vanishes at one loop, we find

$$A_9^Q = +A_{36}^Q + \mathcal{O}(g^4), \quad (87)$$

so long as the W -boson boxes and Z -boson penguins are not taken into account on the SM side (as we have assumed at the very beginning of this section).

Returning to the $b \rightarrow s c \bar{c}$ function, we compare eqs. (69), (70) and (85), and immediately find

$$\begin{aligned} A_1^c &= \frac{g^2}{(4\pi)^2} N_\epsilon^{(1)} \left(-\frac{6}{\epsilon} - 15 - \frac{39}{2}\epsilon \right) + \mathcal{O}(g^4, \epsilon^2), \\ A_2^c &= -1 + \mathcal{O}(g^4), \\ A_{11}^c &= \frac{g^2}{(4\pi)^2} (1 - \epsilon\kappa) \left(-\frac{1}{\epsilon} - \frac{3}{2} \right) + \mathcal{O}(g^4, \epsilon), \end{aligned} \quad (88)$$

which implies that (cf. eqs. (77)–(79) with Z_ψ set to unity)

$$C_1^{c(0)} = 0, \quad C_2^{c(0)} = -1, \quad C_{11}^{c(0)} = 0, \quad (89)$$

and

$$\begin{aligned} C_1^{c(1)} &= N_\epsilon^{(1)} \left(-\frac{6}{\epsilon} - 15 - \frac{39}{2}\epsilon \right) - \frac{1}{\epsilon} C_2^{c(0)} a_{21}^{11} + \mathcal{O}(\epsilon^2) \\ &= -15 + 6\kappa + \epsilon \left(-\frac{39}{2} + 15\kappa - 3\kappa^2 - \frac{1}{2}\pi^2 \right) + \mathcal{O}(\epsilon^2), \end{aligned} \quad (90)$$

$$C_2^{c(1)} = 0, \quad (91)$$

$$\begin{aligned} C_{11}^{c(1)} &= (1 - \epsilon\kappa) \left(-\frac{1}{\epsilon} - \frac{3}{2} \right) - \frac{1}{\epsilon} C_2^{c(0)} a_{2(11)}^{11} + \mathcal{O}(\epsilon) \\ &= -\frac{3}{2} + \kappa + \mathcal{O}(\epsilon). \end{aligned} \quad (92)$$

Indeed, all the $1/\epsilon$ poles have cancelled in the final results for the one-loop Wilson coefficients.

The coefficient C_2^c is the only one that acquires a tree-level contribution in our calculation. For all the other coefficients considered below, we have $C_i^{Q(0)} = 0$.

Let us now turn to the $b \rightarrow s$ *gluon* matching. Comparing eqs. (66)¹² and (83), and

¹² Without S_{13} , since it has been renormalized away by the electroweak counterterm mentioned in the beginning of this subsection.

solving the trivial set of linear equations $\{(84),(86)\}$, one finds

$$\begin{aligned} A_4^c &= \frac{g^2}{(4\pi)^2} N_\epsilon^{(1)} \left(\frac{1}{2} u_2^{(1)} + u_8^{(1)} \right) + \mathcal{O}(g^4, \epsilon^2), \\ A_8^c &= \frac{g^2}{(4\pi)^2} (1 - \epsilon\kappa) \left(\frac{1}{4} u_2^{(1)} + u_{10}^{(1)} \right) + \mathcal{O}(g^4, \epsilon^2), \end{aligned} \quad (93)$$

which implies that (cf. eqs. (77)–(79))

$$\begin{aligned} C_4^{c(1)} &= N_\epsilon^{(1)} \left(\frac{1}{2} u_2^{(1)} + u_8^{(1)} \right) - \frac{1}{\epsilon} a_{24}^{11} C_2^{c(0)} + \mathcal{O}(\epsilon^2) \\ &= \frac{7}{9} + \frac{2}{3}\kappa + \epsilon \left(\frac{77}{54} - \frac{7}{9}\kappa - \frac{1}{3}\kappa^2 - \frac{1}{18}\pi^2 \right) + \mathcal{O}(\epsilon^2), \\ C_8^{c(1)} &= (1 - \epsilon\kappa) \left(\frac{1}{4} u_2^{(1)} + u_{10}^{(1)} \right) + \mathcal{O}(\epsilon^2) \\ &= \frac{1}{3} + \epsilon \left(\frac{11}{18} - \frac{1}{3}\kappa \right) + \mathcal{O}(\epsilon^2). \end{aligned} \quad (94)$$

Similarly,

$$\begin{aligned} C_4^{t(1)} &= (1 - \epsilon\kappa) \left(\frac{1}{2} v_2^{(1)}(x) + v_8^{(1)}(x) \right) + \mathcal{O}(\epsilon^2), \\ C_8^{t(1)} &= (1 - \epsilon\kappa) \left(\frac{1}{4} v_2^{(1)}(x) + v_{10}^{(1)}(x) \right) + \mathcal{O}(\epsilon^2). \end{aligned} \quad (95)$$

Finally, we perform the $b \rightarrow s\gamma$ matching. Comparing eqs. (61), (64) and (81), and solving the trivial set of linear equations $\{(82),(87)\}$, one finds

$$\begin{aligned} A_7^c &= \frac{g^2}{(4\pi)^2} \left[(1 - \epsilon\kappa) \left(\frac{1}{4} h_2^{(1)} + h_{10}^{(1)} \right) + \mathcal{O}(\epsilon^2) \right] \\ &\quad + \frac{g^4}{(4\pi)^4} \left[(1 - 2\epsilon\kappa) \left(\frac{1}{4} h_2^{(2)} + h_{10}^{(2)} \right) + \mathcal{O}(\epsilon) \right] + \mathcal{O}(g^6), \\ A_9^c &= \frac{g^2}{(4\pi)^2} \left[N_\epsilon^{(1)} \left(-\frac{1}{2} h_2^{(1)} - h_8^{(1)} \right) + \mathcal{O}(\epsilon^2) \right] \\ &\quad + \frac{g^4}{(4\pi)^4} \left[N_\epsilon^{(2)} \left(-\frac{1}{2} h_2^{(2)} - h_8^{(2)} \right) + \mathcal{O}(\epsilon) \right] + \mathcal{O}(g^6), \end{aligned} \quad (96)$$

which implies that (cf. eqs. (77)–(80) with Z_ψ and Z_m set to unity)

$$\begin{aligned} C_7^{c(1)} &= (1 - \epsilon\kappa) \left(\frac{1}{4} h_2^{(1)} + h_{10}^{(1)} \right) + \mathcal{O}(\epsilon^2) \\ &= \frac{23}{36} + \epsilon \left(\frac{145}{216} - \frac{23}{36}\kappa \right) + \mathcal{O}(\epsilon^2), \\ C_9^{c(1)} &= N_\epsilon^{(1)} \left(-\frac{1}{2} h_2^{(1)} - h_8^{(1)} \right) - \frac{1}{\epsilon} a_{29}^{11} C_2^{c(0)} + \mathcal{O}(\epsilon^2) \\ &= -\frac{38}{27} - \frac{4}{9}\kappa + \epsilon \left(-\frac{247}{162} + \frac{38}{27}\kappa + \frac{2}{9}\kappa^2 + \frac{1}{27}\pi^2 \right) + \mathcal{O}(\epsilon^2), \end{aligned} \quad (97)$$

and

$$\begin{aligned}
C_7^{c(2)} &= (1 - 2\epsilon\kappa) \left(\frac{1}{4}h_2^{(2)} + h_{10}^{(2)} \right) - \frac{1}{\epsilon} \left[a_{27}^{12}C_2^{c(0)} + (a_{77}^{11} + \beta_0)C_7^{c(1)} + a_{87}^{11}C_8^{c(1)} \right] + \mathcal{O}(\epsilon) \\
&= (1 - 2\epsilon\kappa) \left(\frac{112}{81\epsilon} - \frac{107}{243} \right) - \frac{116}{81\epsilon}(-1) \\
&\quad - \frac{16}{3\epsilon} \left(\frac{23}{36} + \frac{145\epsilon}{216} - \frac{23\epsilon}{36}\kappa \right) + \frac{16}{9\epsilon} \left(\frac{1}{3} + \frac{11\epsilon}{18} - \frac{\epsilon}{3}\kappa \right) + \mathcal{O}(\epsilon) \\
&= -\frac{713}{243} + \frac{4}{81}\kappa + \mathcal{O}(\epsilon), \tag{98}
\end{aligned}$$

$$\begin{aligned}
C_9^{c(2)} &= N_\epsilon^{(2)} \left(-\frac{1}{2}h_2^{(2)} - h_8^{(2)} \right) - \frac{1}{\epsilon^2} (a_{29}^{22} + \beta_0 a_{29}^{11}) C_2^{c(0)} \\
&\quad - \frac{1}{\epsilon} \left[a_{29}^{12}C_2^{c(0)} + a_{19}^{11}C_1^{c(1)} + a_{49}^{11}C_4^{c(1)} \right] - a_{(11)9}^{01}C_{11}^{c(1)} + \mathcal{O}(\epsilon) \\
&= \left[1 - 2\epsilon\kappa + \epsilon^2 \left(\frac{\pi^2}{6} + 2\kappa^2 \right) \right] \left(\frac{128}{81\epsilon^2} + \frac{1496}{243\epsilon} + \frac{5924}{729} + \frac{128}{243}\pi^2 \right) \\
&\quad + \frac{128}{81\epsilon^2}(-1) - \frac{776}{243\epsilon}(-1) + \frac{16}{27\epsilon} \left[-15 + 6\kappa + \epsilon \left(-\frac{39}{2} + 15\kappa - 3\kappa^2 - \frac{1}{2}\pi^2 \right) \right] \\
&\quad - \frac{16}{27\epsilon} \left[\frac{7}{9} + \frac{2}{3}\kappa + \epsilon \left(\frac{77}{54} - \frac{7}{9}\kappa - \frac{1}{3}\kappa^2 - \frac{1}{18}\pi^2 \right) \right] - \frac{64}{27} \left(-\frac{3}{2} + \kappa \right) + \mathcal{O}(\epsilon) \\
&= -\frac{524}{729} - \frac{16}{3}\kappa + \frac{128}{81}\kappa^2 + \frac{128}{243}\pi^2 + \mathcal{O}(\epsilon). \tag{99}
\end{aligned}$$

Again, all the $1/\epsilon^n$ poles have cancelled in the final results.

Similarly, in the top sector we find

$$\begin{aligned}
C_7^{t(1)} &= (1 - \epsilon\kappa) \left[\frac{1}{4}f_2^{(1)}(x) + f_{10}^{(1)}(x) \right] + \mathcal{O}(\epsilon^2), \\
C_9^{t(1)} &= (1 - \epsilon\kappa) \left[-\frac{1}{2}f_2^{(1)}(x) - f_8^{(1)}(x) \right] + \mathcal{O}(\epsilon^2), \\
C_7^{t(2)} &= (1 - 2\epsilon\kappa) \left[\frac{1}{4}f_2^{(2)}(x) + f_{10}^{(2)}(x) \right] - \frac{1}{\epsilon}\gamma_m^{(0)}x\frac{\partial}{\partial x}C_7^{t(1)} - \frac{1}{\epsilon} \left[(a_{77}^{11} + \beta_0)C_7^{t(1)} + a_{87}^{11}C_8^{t(1)} \right] + \mathcal{O}(\epsilon), \\
C_9^{t(2)} &= (1 - 2\epsilon\kappa) \left[-\frac{1}{2}f_2^{(2)}(x) - f_8^{(2)}(x) \right] - \frac{1}{\epsilon}\gamma_m^{(0)}x\frac{\partial}{\partial x}C_9^{t(1)} - \frac{1}{\epsilon}a_{49}^{11}C_4^{t(1)} + \mathcal{O}(\epsilon). \tag{100}
\end{aligned}$$

Here, the x -derivative terms stand for contributions from the top-quark mass renormalization on the full theory side. Instead of including these terms, we could just calculate the corresponding one-loop SM diagrams with counterterm insertions. However, derivatives give us the same results much faster.

It is easy to verify that all the $1/\epsilon$ poles indeed cancel in $C_7^{t(2)}$ and $C_9^{t(2)}$. As usual, the $\mathcal{O}(\epsilon)$ parts of the one-loop Wilson coefficients have affected the results of the two-loop

matching.

The results for $C_2^{c(0)}$, $C_1^{c(1)}$, $C_2^{c(1)}$, $C_4^{Q(1)}$, $C_7^{Q(1)}$, $C_9^{Q(1)}$, $C_7^{Q(2)}$ and $C_9^{Q(2)}$ obtained in the present section have already been summarized in section 2, after passing to the \overline{MS} scheme, i.e. replacing κ by $\ln(M_W^2/\mu_0^2)$. All the other matching conditions summarized there have been found in an analogous manner. In the two-loop Z -penguin contributions to C_9^Q and C_{10}^Q , the effect of renormalizing the $\bar{s}\not{D}b$ term on the SM side was less trivial than in this section. In the two-loop matching for P_1^c and P_2^c , some care was required at renormalizing the top-quark loop contributions in the MOM scheme. In addition, scalar integrals with three non-vanishing masses were necessary [23]. Nevertheless, the basic algorithm remained the same as in the P_7 and P_9 cases, which we have described in detail here.

Summary

We have evaluated two-loop matching conditions for all the operators relevant to $B \rightarrow X_s l^+ l^-$ in the SM. Details of this calculation have been presented only for the operator P_7 and for the photonic penguin contribution to the operator P_9 . As far as the remaining matching conditions are concerned, only the final results have been given. However, the method of the calculation was very similar in all the considered cases.

Our results allowed to remove an important ($\sim \pm 16\%$) uncertainty due to the matching scale μ_0 from the prediction for $BR[B \rightarrow X_s l^+ l^-]$ for low invariant mass of the emitted lepton pair ($\hat{s} \in [0.05, 0.25]$). The obtained Standard Model prediction for the branching ratio integrated over this domain is 1.46×10^{-6} . This result would change to 2.92×10^{-6} if the Wilson coefficient $\tilde{C}_7^{eff}(\mu_b)$ had an opposite sign, as it might happen in certain extensions of the SM.

There remains a sizeable ($\sim \pm 13\%$) perturbative uncertainty in the above SM result, which is due to the unknown two-loop matrix elements of the four-quark operators. Calculable non-perturbative effects which have been included in our result are smaller than this uncertainty. Estimates of other non-perturbative effects suggest that they are not larger. Therefore, the next step in improving the accuracy of the theoretical prediction should be a calculation of the two-loop matrix elements of the four-fermion operators and one-loop matrix elements of the “magnetic moment” ones.

Acknowledgements

We are grateful to Andrzej Buras for suggesting us to work at the matching-scale dependence of $B \rightarrow X_s l^+ l^-$. C.B and J.U. thank Frank Krauss, Klaus Schubert and Gerhard Soff, while M.M. thanks Patricia Ball, Gerhard Buchalla, Paolo Gambino and Frank Krüger for helpful discussions.

This work has been supported in part by the German Bundesministerium für Bildung und Forschung under contracts 06 DD 823, 05 HT9WOA (J.U.) and 06 TM 874 (M.M). M.M. has been supported in part by the DFG project Li 519/2-2, as well as by the Polish Committee for Scientific Research under grant 2 P03B 014 14, 1998-2000.

Appendix

Here, we give the eight evanescent operators that were used in evaluating the anomalous dimension matrices given in section 3. Their explicit form defines what the MS scheme means in the effective theory. As before, the symbol Q stands either for u or for c .

$$\begin{aligned}
P_{11}^Q &= (\bar{s}_L \gamma_{\mu_1} \gamma_{\mu_2} \gamma_{\mu_3} T^a Q_L) (\bar{Q}_L \gamma^{\mu_1} \gamma^{\mu_2} \gamma^{\mu_3} T^a b_L) - 16P_1^Q, \\
P_{12}^Q &= (\bar{s}_L \gamma_{\mu_1} \gamma_{\mu_2} \gamma_{\mu_3} Q_L) (\bar{Q}_L \gamma^{\mu_1} \gamma^{\mu_2} \gamma^{\mu_3} b_L) - 16P_2^Q, \\
P_{15} &= (\bar{s}_L \gamma_{\mu_1} \gamma_{\mu_2} \gamma_{\mu_3} \gamma_{\mu_4} \gamma_{\mu_5} b_L) \sum_q (\bar{q} \gamma^{\mu_1} \gamma^{\mu_2} \gamma^{\mu_3} \gamma^{\mu_4} \gamma^{\mu_5} q) - 20P_5 + 64P_3, \\
P_{16} &= (\bar{s}_L \gamma_{\mu_1} \gamma_{\mu_2} \gamma_{\mu_3} \gamma_{\mu_4} \gamma_{\mu_5} T^a b_L) \sum_q (\bar{q} \gamma^{\mu_1} \gamma^{\mu_2} \gamma^{\mu_3} \gamma^{\mu_4} \gamma^{\mu_5} T^a q) - 20P_6 + 64P_4, \\
P_{21}^Q &= (\bar{s}_L \gamma_{\mu_1} \gamma_{\mu_2} \gamma_{\mu_3} \gamma_{\mu_4} \gamma_{\mu_5} T^a Q_L) (\bar{Q}_L \gamma^{\mu_1} \gamma^{\mu_2} \gamma^{\mu_3} \gamma^{\mu_4} \gamma^{\mu_5} T^a b_L) - 20P_{11}^Q - 256P_1^Q, \\
P_{22}^Q &= (\bar{s}_L \gamma_{\mu_1} \gamma_{\mu_2} \gamma_{\mu_3} \gamma_{\mu_4} \gamma_{\mu_5} T Q_L) (\bar{Q}_L \gamma^{\mu_1} \gamma^{\mu_2} \gamma^{\mu_3} \gamma^{\mu_4} \gamma^{\mu_5} b_L) - 20P_{12}^Q - 256P_2^Q, \\
P_{25} &= (\bar{s}_L \gamma_{\mu_1} \gamma_{\mu_2} \gamma_{\mu_3} \gamma_{\mu_4} \gamma_{\mu_5} \gamma_{\mu_6} \gamma_{\mu_7} b_L) \sum_q (\bar{q} \gamma^{\mu_1} \gamma^{\mu_2} \gamma^{\mu_3} \gamma^{\mu_4} \gamma^{\mu_5} \gamma^{\mu_6} \gamma^{\mu_7} q) - 336P_5 + 1280P_3, \\
P_{26} &= (\bar{s}_L \gamma_{\mu_1} \gamma_{\mu_2} \gamma_{\mu_3} \gamma_{\mu_4} \gamma_{\mu_5} \gamma_{\mu_6} \gamma_{\mu_7} T^a b_L) \sum_q (\bar{q} \gamma^{\mu_1} \gamma^{\mu_2} \gamma^{\mu_3} \gamma^{\mu_4} \gamma^{\mu_5} \gamma^{\mu_6} \gamma^{\mu_7} T^a q) - 336P_6 + 1280P_4.
\end{aligned} \tag{101}$$

References

- [1] Z. Ligeti and M.B. Wise, Phys. Rev. **D53** (1996) 4937.
- [2] A.F. Falk, M. Luke and M.J. Savage, Phys. Rev. **D49** (1994) 3367.
- [3] A. Ali, G. Hiller, L.T. Handoko and T. Morozumi, Phys. Rev. **D55** (1997) 4105.
- [4] J-W. Chen, G. Rupak and M.J. Savage, Phys. Lett. **B410** (1997) 285.

- [5] G. Buchalla, G. Isidori and S.-J. Rey, Nucl. Phys. **B511** (1998) 594.
- [6] G. Buchalla and G. Isidori, Nucl. Phys. **B525** (1998) 333.
- [7] M. Misiak, Nucl. Phys. **B393** (1993) 23, **B439** (1995) 461 (E).
- [8] A.J. Buras and M. Münz, Phys. Rev. **D52** (1995) 186.
- [9] K. Chetyrkin, M. Misiak and M. Münz, Nucl. Phys. **B520** (1998) 279.
- [10] K. Adel and Y.P. Yao, Phys. Rev. **D49** (1994) 4945;
 C. Greub and T. Hurth, Phys. Rev. **D56** (1997) 2934;
 A.J. Buras, A. Kwiatkowski and N. Pott, Nucl. Phys. **B517** (1998) 353;
 M. Ciuchini, G. Degrossi, P. Gambino and G.F. Giudice, Nucl. Phys. **B527** (98) 21;
 C. Bobeth, M. Misiak and J. Urban, hep-ph/9904413, to appear in Nucl. Phys. **B**.
- [11] M. Misiak and J. Urban, Phys. Lett. **B451** (1999) 161.
- [12] G. Buchalla and A.J. Buras, Nucl. Phys. **B400** (1993) 225.
- [13] G. Buchalla and A.J. Buras, Nucl. Phys. **B548** (1999) 309.
- [14] K. Chetyrkin, M. Misiak and M. Münz, Phys. Lett. **B400** (1997) 206,
B425 (1998) 414 (E).
- [15] Particle Data Group, Eur. Phys. J. **C3** (1998) 1.
- [16] F. Krüger and L.M. Sehgal, Phys. Lett. **B380** (1996) 199.
- [17] N. Cabibbo and L. Maiani, Phys. Lett. **B79** (1978) 109.
- [18] Y. Nir, Phys. Lett. **B221** (1989) 184.
- [19] C.W. Bauer and C.N. Burrell, hep-ph/9907517.
- [20] A. Ali and G. Hiller, Phys. Rev. **D58** (1998) 074001;
 G. Hiller, hep-ph/9809505.
- [21] P. Cho, M. Misiak and D. Wyler, Phys. Rev. **D54** (1996) 3329.
- [22] J. Küblbeck, M. Böhm and A. Denner, Comput. Phys. Commun. 60 (1990) 165.
- [23] A.I. Davydychev and J.B. Tausk, Nucl. Phys. **B397** (1993) 123.
- [24] A.J. Buras and P.H. Weisz, Nucl. Phys. **B333** (1990) 66;
 M. J. Dugan and B. Grinstein, Phys. Lett. **B256** (1991) 239;
 S. Herrlich and U. Nierste, Nucl. Phys. **B455** (1995) 39.
- [25] K. Chetyrkin, M. Misiak and M. Münz, Nucl. Phys. **B518** (1998) 473.